Crankpin Bearings in High Output Aircraft Piston Engines

The Evolution of their Design and Loading

by Robert J. Raymond

July 2015

Abstract

The development of the crankpin bearing in high output aircraft piston engines is traced over the period 1915-1950 in a large number of liquid and air cooled engines of both American and European origin. The changes in bearing dimensions are characterized as dimensionless ratios and the resulting changes in the associated weights of rotating and reciprocating parts as weight densities at the crankpin. Bearing materials and developments are presented to indicate how they accommodated increasing bearing loads.

Bearing loads are characterized by maximum unit bearing pressure and minimum oil film thickness and plotted as a function of time. Most of the data was obtained from the literature but some results were calculated by the author. A technique for evaluating bearing loads is presented for both in-line, V and W engines as well as radial engines of seven and nine cylinders per row.

Among the results presented are comparisons of the crankpin bearing loads in the Rolls-Royce Merlin and the Allison V-1710 and the unique approaches taken by the Bristol Aeroplane Company's Engine division to solve some of the design problems associated with crankpin bearings.

Preface

If a need for a device persists, its design inevitably evolves. This evolution is driven by technology and the purpose the device serves. Simple hand tools change to accommodate an improved understanding of how the human body and the tool interact and to incorporate new materials and manufacturing techniques. Buildings change under the influence of new materials and advances in computer aided design and computer aided fabrication techniques. Many modern buildings would have been impractical prior to the age of computers. The automobile is an excellent example of a machine that has evolved to a level of global uniformity in both design and technology. Fifty or sixty years ago an automobile's country of origin was obvious from its appearance. British, French, German, Italian and American cars were distinctive and easily identifiable. A 1960 Oldsmobile could only have been American and a Citroen 2CV could only have been French to anyone even remotely interested in cars. Today one would be very hard pressed to define the national characteristics of most mass produced automobiles.

The high output aircraft piston engine is a rather unique example of a machine that, despite 40 years of intense development, did not achieve an advanced state of evolution before being abruptly eclipsed by the gas turbine. It had certainly not arrived at the kind of technical consensus we see when we look under the hood of a long haul Diesel powered truck. There you will invariably find a 6-cylinder, 4-stroke cycle, open chamber, turbocharged, aftercooled engine with electronically controlled fuel injection. Gone are the two-stroke cycle, divided combustion chambers, and the many variants of mechanical injection systems found in truck engines of the past.

At the end of the large piston engine era there was still a broad spectrum of engine configurations being produced and actively developed. Along with the major division between liquid and air-cooled engines there was a turbo-compounded engine, a four-row air-cooled radial engine, engines with poppet valves and engines with sleeve valves, all in production. There were also a two-stroke turbo-compounded Diesel engine, a 2-stroke spark ignition sleeve valve engine and engines with unusual cylinder arrangements all under development, to mention only a few. This plethora of options was largely due to difficulties in achieving with piston engines the power requirements of ever larger aircraft.

The specific output of both air-cooled and liquid-cooled aircraft engines increased from about one horsepower per square inch of piston area to around seven or eight in the period from WWI to the end of WWII. Despite this remarkable increase in output the physical size of the engines did not change much when corrected for bore size, and the weight per cubic inch of displacement increased from approximately 0.45 to 1.1, or less than a factor of three. This accomplishment testifies to the intense effort that went into all aspects of aircraft engine development. A short list of critical areas that were addressed to reach this level of performance could include the following:

- Producing durable exhaust valves
- Controlling crankshaft torsional vibration
- Designing efficient superchargers
- Sealing combustion chambers effectively
- Improving air-cooled cylinder cooling fins
- Improving bearing materials

This paper will focus on the evolution of the crankpin bearing over the time period from 1915 to 1950. This approach has the advantage of being amenable to a quantitative description of the changes over time that are fairly well described in the literature. Support for bearing research and development by the U.S. government indicates how important this aspect of aircraft engine development was. Work on bearings began at McCook Field in the early 1920s and continued there and at Wright Field. The National Advisory Committee for Aeronautics (NACA) sponsored analytical and experimental work on journal bearings until well after WWII. That this work was crucial is demonstrated by the fact that all of the high output engines of the WWI

era had unit crankpin bearing loads that exceeded the capacity of the bearing materials and/or the fabrication techniques available at that time. Without this large body of work in the public realm this paper would have been very difficult to write.

Present day motor vehicles are remarkably free of bearing failures but this has not always been the case. As a teenager interested in engines I learned how to distinguish between a "rod rap" and a "main bearing thud" because these were common problems one had to be aware of when purchasing an old car. On the extremely rare occasions when I do hear these sounds again I wonder at what kind of abuse that engine must have suffered. Auto mechanics will testify to the rarity of bearing failures not attributable to some form of abuse (such as NASCAR racing). This was not the case in the early days of aircraft engines. Bearing problems were endemic and continued to be so for many years. The absence of problems in today's motor vehicles is in good measure due to insights and materials developed during the high output aircraft piston engine era.

Despite the large specific output increase, the ratio of bearing projected area (length x diameter) to piston area increased, on average, by only 15% for air-cooled engines and actually decreased by about 8% for in-line V configurations. This achievement was due to a better understanding of hydrodynamic lubrication in journal bearings and a very intense development effort in bearing materials, their design and fabrication. Despite these advances, journal bearings were not universally adopted. Rolling element bearings were utilized in the main bearing positions in many radial engines to the end of the era. One in-line V engine, the Daimler-Benz DB601, used a rolling element bearing in the crankpin position, another indication of immature evolution.

This paper is concerned with how mean and maximum unit bearing loads increased and how the bearing dimensions and materials evolved to cope with them. I will not get into the details of bearing chemistry and the very complex techniques required to disperse critical additives into the basic bearing material. The technique of bearing load evaluation is not discussed in great detail since there are many good references available. The information presented here is arranged in a way that allows the reader to evaluate the mean and maximum bearing loads for any in-line, V, or W engine and any 7 or 9-cylinder radial engine with a knowledge of the basic engine dimensions, the imep and the reciprocating and rotating weights at each crankpin.

Mean and maximum bearing loads are presented for a significant number of engines, both in-line, V, W and radial engines from WWI to the end of the era of the high output piston aircraft engine. The manner in which the bearing dimensions changed with time and trends in various parameters pertaining to hydrodynamic lubrication are also presented.

Introduction

Figure 1 shows V and radial engine connecting rod arrangements prevalent in the period under discussion. In-line engines used the same arrangement prevalent today in automotive practice. Some V and W configurations used the radial engine's articulated arrangement rather than the fork and blade arrangement, but by the end of the piston engine era most manufacturers used the arrangements shown in Figure 1, Hispano–Suiza being a notable exception. From this point onward, V, W, and in-line engines will be referred to as in-line unless the discussion requires that the type be specified.

Both the V- fork and blade connecting rod and the one piece master rod of Figure 1 are later designs and represent a high level of refinement. Many early radial engines had split big-end master rods with one-piece crankshafts, and this arrangement persisted in some engines until the end of the era. Figure 1 also shows a typical arrangement of a split master rod.

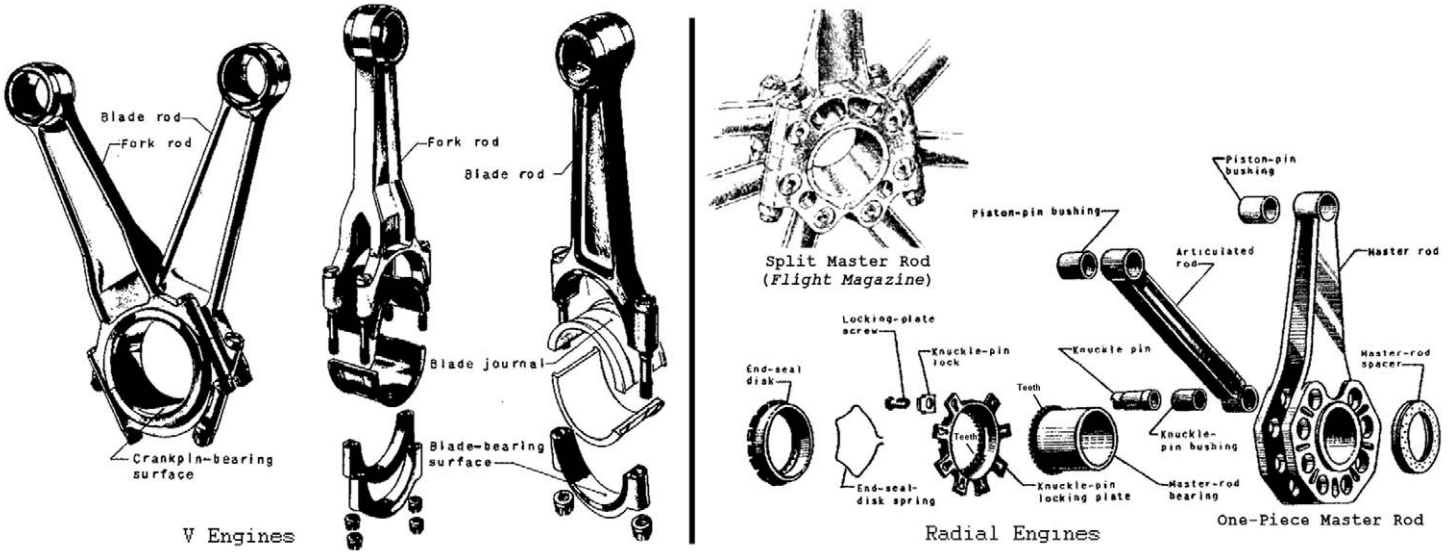

Figure 1. Connecting Rod Arrangements (NACA)

It is important to note that in V engines the blade rod loads are transmitted to the crankpin journal surface and the blade rod journal bearing surface is on the outer diameter of the crankpin bearing, which, in turn, is clamped in the fork rod. This results in the blade journal operating in an oscillatory motion similar to that of the wrist pin. Unlike the crankpin bearing, neither of these bearings is completely hydrodynamic. Similarly, the articulated rod bearings in the radial configuration are not hydrodynamic and, in addition, impose a bending moment on the master rod that is absent in the fork and blade arrangement.

When journal bearings are utilized in the crankshaft main bearing positions, they operate as fully hydrodynamic bearings. The problem with using these bearings to characterize the evolution of bearing loading is the difficulty in evaluating the loads since, in the case of in-line engines or multi-row radials, loads are coming from adjacent cylinders or rows of cylinders. In addition, the relative stiffness of the crankshaft and the crankcase can allow bending and deflections that result in non-uniform loading of the bearing surface. The presence of counterweights also adds to the complexity. For these reasons and the fact that many radial engines had rolling element bearings in the main bearing positions, I have opted to use the crankpin bearing as the characteristic bearing in the load path from cylinder pressure to torque at the propeller.

In this analysis two variables will be used to characterize bearing loads, the maximum unit bearing pressure and the mean unit pressure as expressed in the Sommerfeld Number, which characterizes the minimum oil film thickness at the bearing. By unit pressure I mean the load on the bearing divided by the projected area of the bearing (length x diameter). Bearings that operate with cyclical loads per revolution fail either due to fatigue of the bearing material (high maximum unit pressure) or because the minimum film thickness is less than required for hydrodynamic lubrication, resulting in increased friction. The minimum film thickness is influenced by the rotating speed and the mean unit bearing pressures. For the purposes of this analysis I am assuming that the minimum film thickness is a function of the mean unit pressure and is little influenced by the maximum unit pressure, which occurs very briefly. A comparison of this approach with an exact solution from Reference 1 for the Wright R-1820 engine at 2,500 rpm and 245 psi imep gave good agreement.

It should be recognized that bearings often fail for other reasons: high temperature due to inadequate oil flow, dirt, misalignment, cavitation, etc. The representation I have chosen to use here is a simplification of the actual situation in an engine bearing but is a convenient way to compare the bearing loads in a number of engines over an historical time period, which is the purpose of this paper. It should also be recognized that the maximum oil pressure in the film of a hydrodynamically loaded bearing is much higher than the mean or maximum unit pressures by as much as an order of magnitude. The maximum load capacity of bearing materials during the time period under consideration here was expressed in terms of unit pressure. The minimum oil film thickness below which bearing friction increases rapidly was based on a minimum Sommerfeld number, which varies inversely with mean unit bearing pressure, an acceptable value being dependent on bearing material and the detailed design of the bearing.

In what follows, we will examine how the crankpin design evolved over time for both in-line and radial engines. This will be characterized by the design ratios; crankpin diameter to bore and length to crankpin bearing diameter. The effective rotating mass at the crankpin to give the mean inertia load on the bearing will also be presented.

Maximum bearing pressures will be shown for a number of engines together with the accepted load capacities of the bearing materials used throughout the period. A minimum oil film thickness will be characterized for these engines based on the mean bearing load.

The final section of this paper will present a technique for evaluating mean and maximum bearing loads based on a dimensional analysis technique developed by Shaw and Macks (1) and expanded by the author to include in-line, V, and W engines.

Trends in Bearing Design

Tables 1 and 2 show crankpin bearing dimensions and weights of the reciprocating and rotating parts of the engines evaluated in this paper. The sources of this data are given in the tables. These tables also serve to define the nomenclature used in the Figures that follow.

Figure 2 shows how the fundamental bearing dimensions changed over time for in-line, V and W engine configurations listed in Table 1. It should be noted that the dates given in the tables, which are primarily from (2) and (3), are for the year the engine was designed and do not necessarily correspond to the dates on the Figures, which represent the dates for which the data given was available. This will be the case throughout this paper. While the fundamental dimensions seldom changed, the weights of the reciprocating and rotating parts did change as did the imep and these changes had an impact on bearing loads.

The points of interest in Figure 2 are:

- The wide range of design ratios in the WWI era and subsequent convergence on a consensus value at the end of the era.
- In the WWI era there appears to have been some consensus as to what the bearing area should be but no agreement as to the "correct" value of length to diameter ratio. The large diameter bearings are short and vice-versa.
- The abrupt change in bearing area of the Curtiss V-1570 as compared to the D-12 and K-12. The effect of this rather radical change will be discussed in the section devoted to maximum bearing pressure.
- The Rolls-Royce Eagle 22 diverges dramatically because sleeve valve porting increases cylinder spacing as compared to poppet valve engines. See Ref. 32 Table 2.

Table 1. In-Line, V, and W Engine Dimensions, Reciprocating and Rotating Weights

Engine Configuration Year Designed	Bore B (in)	Stroke L (in)	Cylinders n	Cylinders per row n′	Crankpin Diameter D_{CP} (in)	Effective Crankpin Bearing Length ℓ_{CP} (in)	Con-Rod Length ℓ_{CR} (in)	Recip. Weight per Cylinder W_{RCP}/CYL (lb)	Rotating Weight W_{ROT} (lb)	Compression Ratio r	Remarks
1. Rolls-Royce Eagle 22 Flat H - 2 Cranks	5.400	5.125	24	2 per crank	2.904	2.450	10.25	—	—	7.00	Diameter from Ref. 12 ℓ_{CP} from Barry Hares
2. Rolls-Royce Griffon 60° V-12 1939	6.000	6.600	12	2	3.100	2.030	10.65	6.28	8.08	6.00	Dimensions - Ref. 13 Weights - See Note 1 below
3. Rolls-Royce Merlin 60° V-12 1933	5.400	6.000	12	2	2.774	2.000	10.10	5.69	5.93	6.00	D_{CP} from Ref. 14 ℓ_{CP} scaled (est) (see note 2 below)
4. Junkers-Jumo 211 B Inverted 60° V-12 1933	5.900	6.500	12	2	2.990	1.824	11.01	8.47	7.63	7.00	Dimensions & Weights - Ref. 15
5. Allison V-1710 60° V-12 1930	5.500	6.000	12	2	3.000	1.940	10.00	6.72	7.91	6.65	Dimensions & Weights - Ref. 1
6. Rolls-Royce Kestrel 60° V-12 1926	5.000	5.500	12	2	2.500	1.800	9.27	3.90	4.30	6.00	ℓ_{CR} Value is scaled from Merlin. Dimensions and weights from Ref. 5
7. Curtiss V-1570 60° V-12 1924	5.125	6.250	12	2	2.500	1.390	10.00	4.01	5.36	5.80	Dimensions & Weights - Ref. 4
8. Curtiss D-12 60° V-12 1922	4.500	6.000	12	2	2.500	1.812	10.02	3.25	5.10	5.30	Dimensions & Weights - Ref. 6
9. Napier Lion W-12 1916	5.500	5.125	12	3	2.750	2.625	9.74	5.50	6.40	5.80	Dimensions & Weights - Ref. 4
10. Hispano-Suiza 300 90° V-8 1916	5.510	5.910	8	2	2.130	2.444	10.37	7.20	6.20	5.30	Dimensions & Weights - Ref. 6
11. Curtiss K-12 60° V-12 1916	4.500	6.000	12	2	2.500	1.875	10.38	3.25	4.40	5.30 (est)	Dimensions & Weights - Ref. 6
12. Liberty-12 45° V-12 1917	5.000	7.000	12	2	2.375	2.187	12.22	6.20	6.30	5.40	Dimensions & Weights - Ref. 5
13. Rolls-Royce Eagle 60° V-12 1915	4.500	6.500	12	2	2.250	1.880	12.22	3.75	3.95	6.00	Dimensions & Weights - Ref. 6
14. Maybach Inline 6 ca. 1916	6.500	7.090	6	1	2.600	2.660	12.19	17.35	5.63	5.95	Dimensions & Weights - Ref. 4
15. Austro-Daimler Inline-6 1916	5.315	6.890	6	1	2.200	2.280	12.40	5.84	3.18	5.02	Dimensions & Weights - Ref. 16

Note 1: Piston Assembly Weight from Brian Mills; Rod Weights & Distribution from Tom Fey.

Note 2: The total weight of the connecting rod and the piston assembly were provided by a reputable rebuilder of Merlin engines.The distribution of weights between reciprocating and rotating is the author's estimate.

Table 2. Radial Engine Dimensions, Reciprocating and Rotating Weights

Engine Year Designed	Bore B (in)	Stroke L (in)	Cylinders n	Cylinders per row n′	Crankpin Diameter D_{CP} (in)	Effective Crankpin Bearing Length ℓ_{CP} (in)	Master Rod Length ℓ_{CR} (in)	Recip. Weight per Cylinder W_{RCP}/CYL. (lb)	Rotating Weight W_{ROT} (lb)	Compression Ratio r	Remarks (Weights are for year of rating in Table 4)
1. Wright R-1820 1931	6.125	6.875	9	9	3.25	3.10	13.750	8.93	32.72	6.80	Weights - Ref. 1
2. Pratt & Whitney R-2800 1936	5.750	6.000	18	9	3.50	3.06	12.310	8.24	34.57	6.75	Dimensions & Weights - Ref. 1 One piece master rod
3. Wright R-3350 1936	6.125	6.313	18	9	3.63	3.03	13.940	8.57	33.96	6.85	Dimensions & Weights - Ref. 1 One piece master rod
4. Pratt & Whitney R-1830 1931	5.500	5.500	14	7	2.62	3.63	10.280	6.76	28.17	6.70	Dimensions & Weights - Ref 1 Split master rod
5. Wright R-2600 1935	6.125	6.313	14	7	3.63	2.80	14.110	8.66	28.89	6.90	Dimensions & Weights - Ref. 1 One piece master rod described in 1941
6. Armstrong-Siddeley Jaguar V 1917	5.000	5.500	14	7	2.50	3.80	10.370	3.71	12.80	5.00	Dimensions & Weights - Ref. 5 Split master rod
7. Bristol Jupiter IV 1924	5.750	7.500	9	9	2.12	3.95	12.860	4.48	18.86	5.00	Dimensions & Weights - Ref. 5 Split master rod
8. Wright R-1750 1926	6.000	6.875	9	9	3.25	3.56	13.750	6.82	25.22	5.00	Dimensions & Weights - Ref. 4 One piece master rod
9. Bristol Jupiter VIII 1928	5.750	7.500	9	9	2.25	3.11	12.860	4.66	17.30	6.30	Dimensions & Weights - Ref. 5 One piece master rod
10. Armstrong-Siddeley Tiger 1930	5.500	6.000	14	7	3.00	3.47	10.500 (est.)	5.73	25.1	5.20	Weights & Dimensions - Ref. 5 Split master rod
11. Armstrong-Siddeley Panther 1928	5.250	5.500	14	7	2.75	3.35	10.300 (est)	4.36	19.52	5.0 ?	Weights & Dimensions - Ref. 5 Split master rod
12. Wright Fictional "R-1418"	6.125	6.875	7	7	–	–	13.750	8.93	28.28	6.80	Fictional. Seven R-1820 Cylinders for Bearing Load Comparison. See Table 6.
13. Bristol Jupiter VI 1926	5.750	7.500	9	9	2.25	3.19	12.860	4.48	17.47	5.3 ? 6.3 ?	Dimensions & Weights - Ref. 5 Engine offered at both compression ratios, but Ref. 5 does not specify which.
14. Pratt & Whitney R-1340 1925	5.750	5.750	9	9	2.63	3.38	12.600 (est.)	6.28	19.80	5.25	Weights & Dimensions - Ref. 4 One piece master rod
15. Pratt & Whitney R-1860 1929	6.250	6.750	9	9	2.88	3.50	13.700 (est.)	7.93	28.18	5.00 ?	Weights & Dimensions - Ref. 4
16. Bristol Pegasus 1930	5.750	7.500	9	9	2.69	2.92	13.365 (est)			6.55	Piston Assembly - 1910g (from R-RITT)
17. Bristol Hercules 1934	5.750	6.500	14	7	3.07	2.91	14.038 (est)	7.38	–	7.00	Reciprocating Weight per Cylinder from Brian Mills
18. Bristol Centaurus 1937	5.750	7.000	18	9	3.79	3.19	14.850	7.98	32.89	7.20	Weights from Brian Mills Dimensions - Ref. 17

Figure 3 gives the same design ratios for the radial engines listed in Table 2. The same convergence on a consensus evident in Figure 2 is present here as well and the lack of consensus circa 1925 parallels the situation with in-line engines circa 1916. For its time, the Armstrong-Siddeley Jaguar seems to have struck the right balance

The trend to shorter bearings in both in-line and radial engines was due to the following:

- A desire to minimize the effects of crankshaft and crankcase deflections on bearing misalignment and consequent bearing wear.
- Improved oil flow through the bearing without resorting to excessive oil pressure.
- Reduced engine length.
- In the case of in-line engines the longer bearings necessitated the use of four big end bolts, which increased the inertia load on the bearing; both the Austro-Daimler and Maybach engines of Table 1 had four bolt big-ends.

Figure 4 shows the weight density at the crankpin for in-line and radial engines versus time. This weight, which results in giving the mean inertia load at the crankpin, is a function of the reciprocating and rotating weights and is

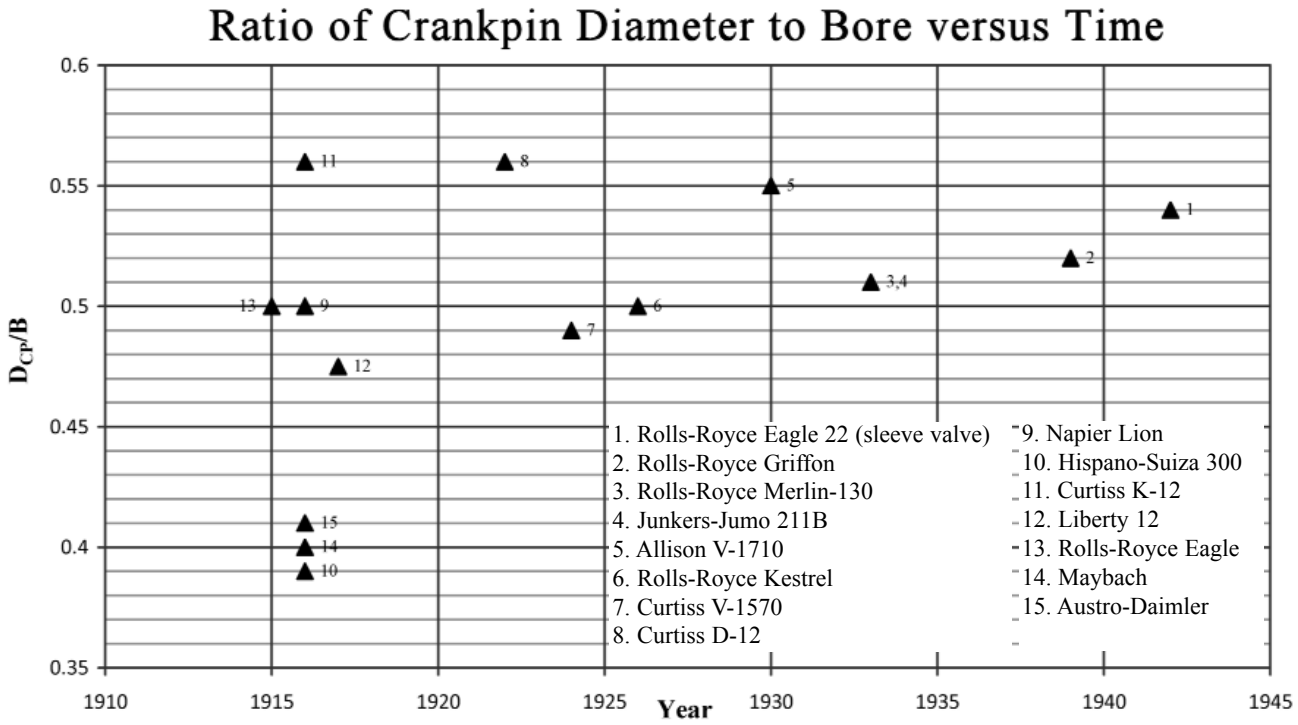

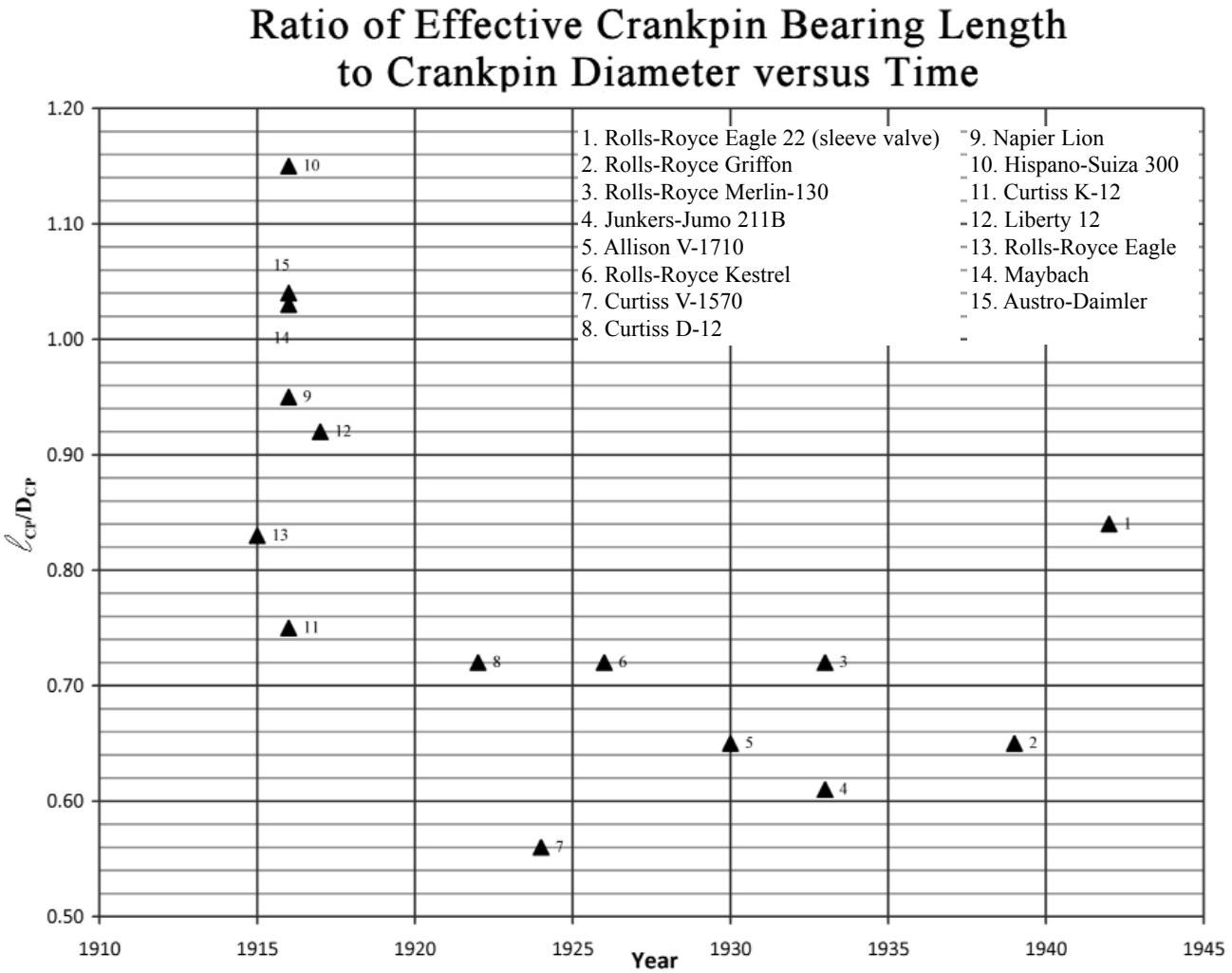

Figure 2. Crankpin Dimension Ratios, In-Line, V and W Engines

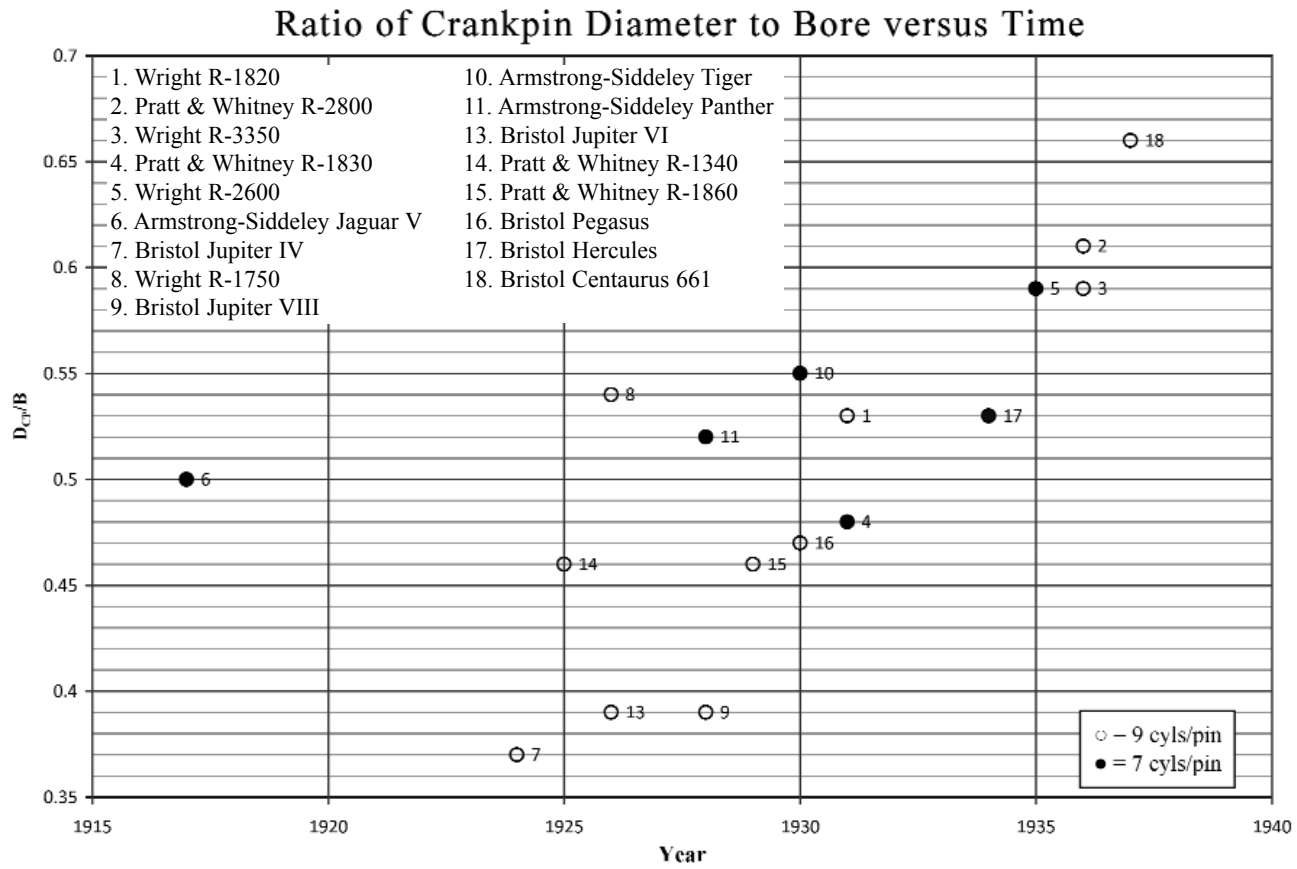

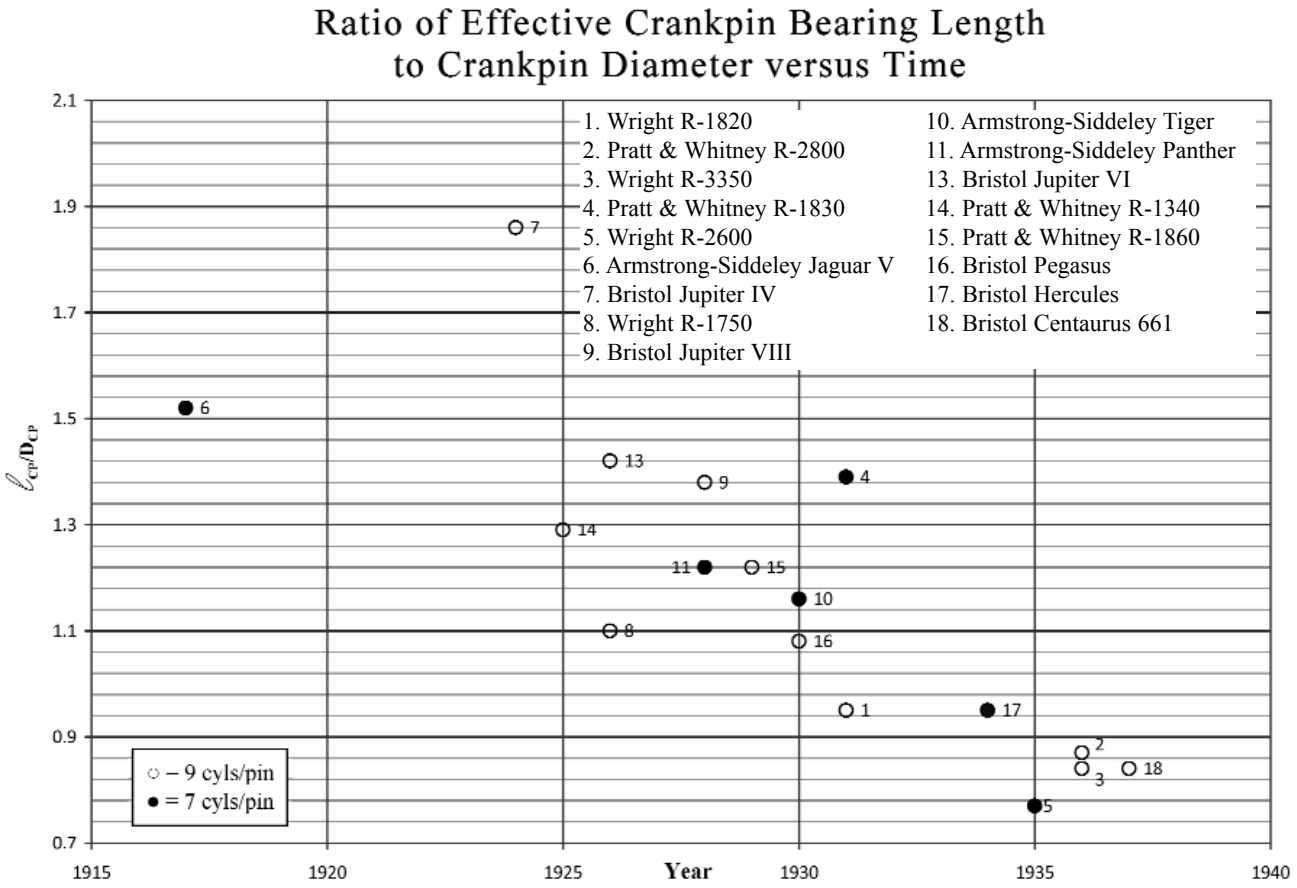

Figure 3. Crankpin Dimension Ratios, Radial Engines

defined in Figure 27. We see a wide spread in the weight density in the early in-line engines and a gradual convergence. I have shown the final weights for engines designed much earlier but there is insufficient information to show how these weights might have evolved over the time period. It is interesting to note that the Liberty 12 has the highest weight density while its crankpin diameter and bearing length are in the mid-range of Figure 2.

Unlike in-line engines, which do not show much of an increase in weight density with time, the radial engines do show an increase. This can be traced back to Figure 3, where the ratio of crankpin diameter to bore increased significantly with time. Note that the ratio of the weight densities is about a factor of 4, radial to in-line. As we shall see this implies a much higher mean bearing load for radial engines and is the reason the bearing area had to increase, leading to larger crankpin diameters.

We can see the effect of the split master rod on the weight density if we compare the Wright R-2600 (one-piece master rod) and the Pratt & Whitney R-1830 (split master rod) in Figure 4. Table 2 indicates about the same rotating weights for these two engines despite the larger bore and crankpin diameter of the R-2600, resulting in a weight/density ratio about 22% higher for the R-1830. The same effect is seen in the three Bristol Jupiter engines in Figure 4 (engines 7, 9 and 13). The Jupiter IV (engine 7) had a smaller crankpin diameter and a split master rod (see Table 2) but was slightly heavier than the other two.

It is evident that the earlier Bristol engines were designed on the light side but became relatively heavier as Figure 4 clearly indicates. The weight of a Bristol Pegasus (model unknown) piston was recently obtained through the R-RHT (Bristol Branch) and its weight was about 63% of the Pratt & Whitney R-2800 assembly. Reference 18 gives the weights of Perseus XII and Hercules X piston assemblies ca.1943 and they are 74% and 81% of the R-2800 assembly. The weights of late model Hercules and Centaurus assemblies were provided by Brian Mills and they were 89% and 92%of the R-2800 weight. All four engines had 5.75" bores.

Bearing Materials 1915-1950

Early crankpin bearings were almost universally tin based Babbitt (white metal) and were either poured directly into the connecting rod or a bronze shell was used. Babbitt composition in the WWI era was typically 80% tin, 12% antimony and the remainder copper and lead. Modern tin based Babbitt is closer to 90% tin with the remainder copper, antimony and lead (S.A.E. 10, 11, 12).

The blade rod journal was the outer diameter of the bronze shell. The thickness of the Babbitt on the inner diameter of the shell (or directly on the rod) was typically excessive and contributed to the poor fatigue life of the bearing. The bronze shell apparently would become loose due to differential expansion (Heron, 19). Since bronze has a higher coefficient of expansion than steel, the shell must have yielded to cause it to become loose. Aside from a Reference by Heron to some bearings made by Bugatti for the Liberty engine during WWI, which utilized a steel shell with a thin layer of Babbitt on the inner diameter, it wasn't until the early 1920s that significant advances in bearing materials and construction were made.

It is unclear where the idea for the steel backed bearing originated in the U.S. Heron credits Gilman at Allison while Whitney (20) credits Army Air Corp engineers who then approached Allison for help. In any case, Allison developed a bearing with a steel shell, a thin Babbitt lining and a bonded copper-lead alloy on the outer diameter to serve as a bearing surface for the blade rod. The copper-lead blade bearing surface worked so well that it was adopted as the inner bearing material as well, replacing the Babbitt. The development of the manufacturing procedures for the new bearings was largely due to Allison. This was a difficult task, primarily to get the chemistry right and to get good distribution of lead particles in the spongy copper matrix. A representative copper-lead bearing toward the end of the period under consideration here would have been 69% copper, 30% lead and 1% silver on a steel backing. The copper/lead was typically 0.03 ~ 0.04" thick (Reference 1). Corrosion of the lead by acids in the lube oil was alleviated by oil additives and the addition of small amounts of indium to the bearing material.

The copper/lead bearing was satisfactory for many years but by the mid 1930s the crankpin bearing loads in some radial engines began to exceed their capacity. Hobbs of Pratt & Whitney is credited with the next major advance in bearing materials (Reference 21). Hobbs proposed silver and lead as a bearing material, silver for its fatigue strength and high thermal conductivity and lead for its resistance to scoring and embeddability. Testing of the new material was very successful but there were sporadic failures due to lead corrosion. This problem was also solved by the addition of indium. The final configuration, according to Reference 1, was a 0.02 ~ 0.03" layer of silver electroplated to a soft steel shell with a thin layer of lead 0.001 ~ 0.003" thick on the silver with indium at 4% by weight of the lead. This bearing was used in both radial and in-line V engines during WWII.

It is obvious that creating these bearings was an art: getting the proper chemistry, distributing the various materials in each other and getting them to bond to each other and the steel shell was a long and arduous process to which this brief description does not do justice. When the bearing shell is fitted to the connecting rod in the case of split big ends the two halves of the bearing are not circular and are deformed by the rod when clamped together so that there is good contact between the shell and the connecting rod. It also took a great deal of development to get interchangeable bearings that did not require a finishing operation after installation in the rod. Heron (19) claims that Pratt & Whitney was the first to make interchangeable split bearing shells and that this was achieved by "being distorted in the boring fixture so that they were neither parallel nor round when removed from the fixture. This was done so that

when the bearing was under load and clamped in the split master rod, the bearing showed no high spots under load." With only 0.001 ~ 0.003" of lead on the surface of the silver/lead bearing any final sizing of the bearing clearance after installation would be very difficult.

Maximum Unit Bearing Pressures

Maximum unit bearing pressures versus time for in-line, V, W, and radial engines are shown in Figure 5. The nominal fatigue strength of the various bearing materials is also shown. These fatigue strengths are a function of their operating temperature, in this case 300° F (1).

Tables 3 and 4 give the engine ratings for these points and the bearing loads corresponding to the unit pressures. The source of the data is also given in the tables. It should be kept in mind that these pressures are at the max power or

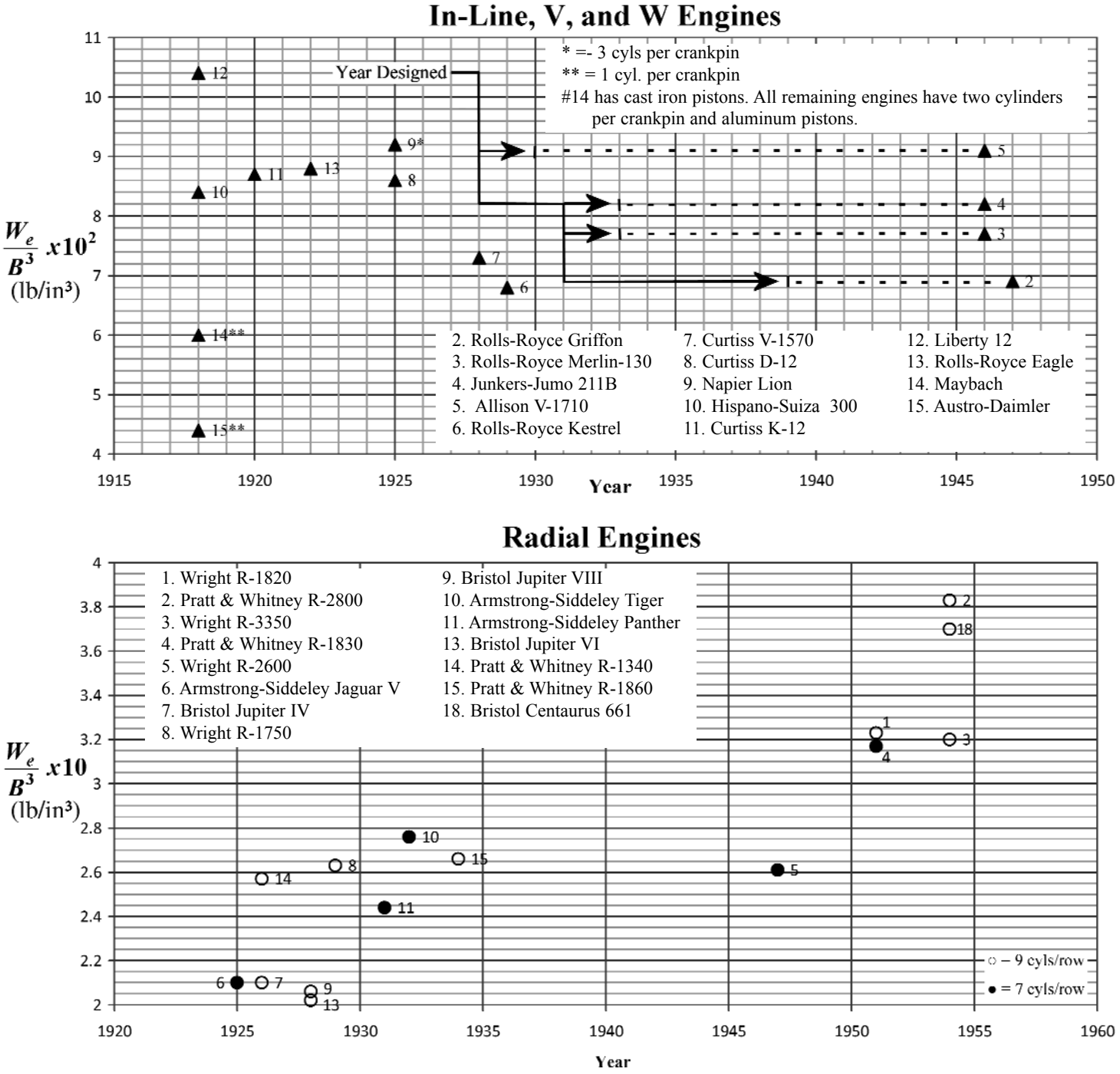

Figure 4. Weight Density at Crankpin versus Time

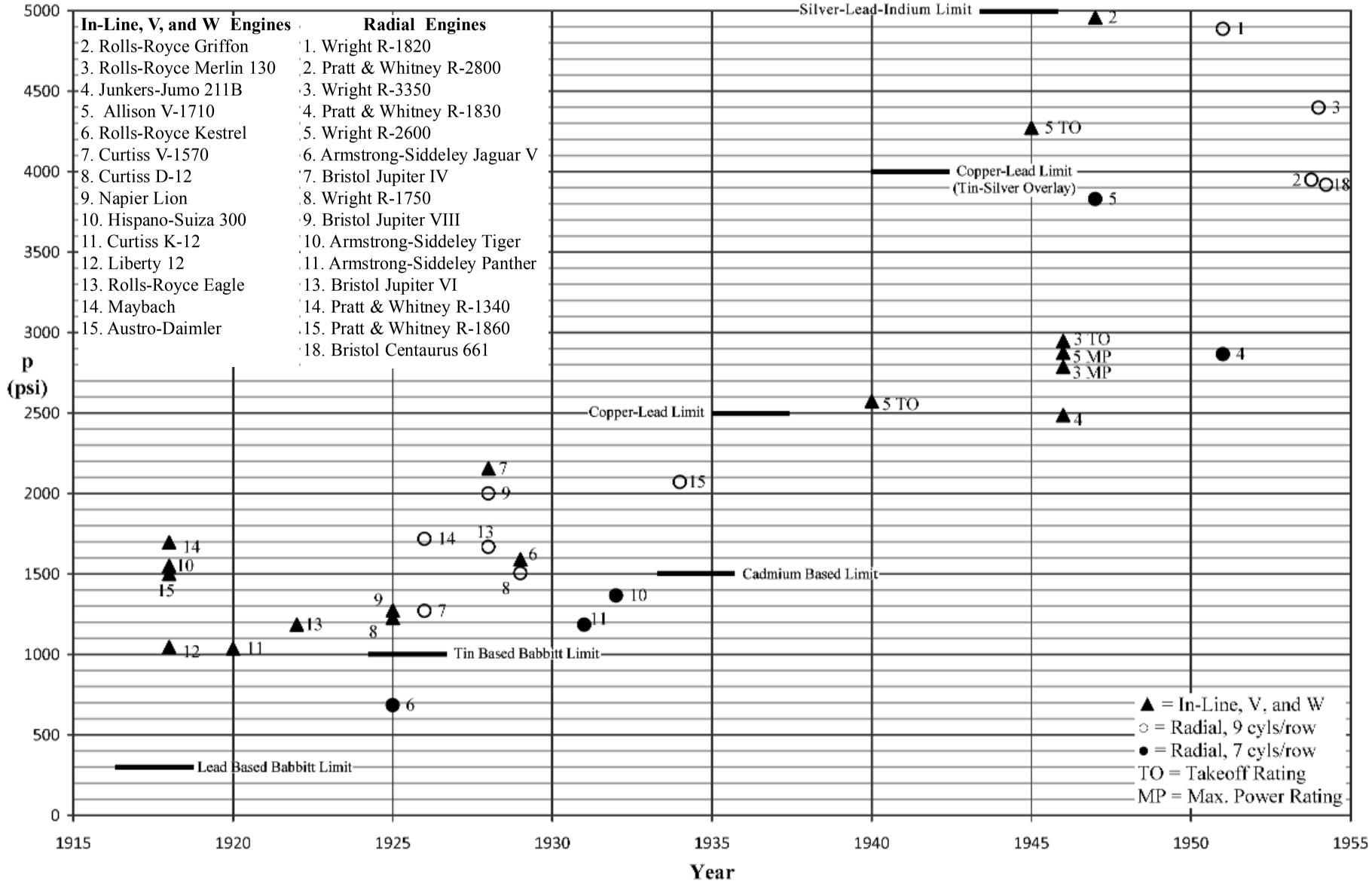

Figure 5: Maximum Crankpin Unit Bearing Pressure versus Time, Various Engines

Table 3. In-Line, V, and W Engine Ratings and Bearing Loads

Engine (Year of Rating)	Brake Horsepower BHP	Engine Speed N (RPM)	Brake Mean Effective Pressure BMEP (psi)	Indicated Mean Effective Pressure IMEP (psi)	Maximum Bearing Load W (lb)	Mean Bearing Load $\bar{W}$ (lb)	Maximum Bearing Pressure p (psi)	Mean Bearing Pressure $\bar{p}$ (psi)	Oil Temperature T_{oil} (°F)	Oil Viscosity μ (lb-sec/in^2 x 10^6)	Oil Specific Gravity ρ (g/cm^3)	Sommerfeld Number S —	Eccentricity Ratio n —	Minimum Oil Film Thickness h_{min} (in x 10^4)	Remarks
1. Rolls-Royce Eagle 22 (1947)	3500	3500	281	—	—	—	—	—	—	—	—	—	—	—	No weights available to author.
2. Rolls-Royce Griffon (1947)	2420	2750	311	404	31197	12217	4957	1941	185°	4.00	0.86	0.168	0.64	4.24	Bearing Loads by Author using Figs. 13 & 14 for mean loads and standard method for maximum loads
3. Rolls-Royce Merlin 130 (1946, Take-off)	1645	3000	263	336	18853	10092	3398	1819	185°	4.00	0.86	0.193	0.60	4.20	
4. Junkers-Jumo 211B (1946)	1200	2400	186	228	16431	9524	3019	1746	170°	5.50	0.86	0.224	0.64	4.00	
5. 5. Allison V-1710 (1946, Max Power)	1361	3000	210	278	16735	12278	2875	2110	185°	4.00	0.86	0.168	0.65	3.66	Bearing Loads - Ref. 1
6. Rolls-Royce Kestrel (1929)	550	2500	134	156	7155	4455	1590	990	140°	10.16	0.88	0.760	0.23	7.30	Bearing Loads - Ref. 5
7. Curtiss V-1570 (1928)	630	2400	132	148	7070	5200	2155	1585	150°	8.22	0.87	0.369	0.47	5.00	Effective Bearing Area = 3.28 in^2 due to oil groove. Bearing loads - Ref. 4
8. Curtiss D-12 (1925)	462	2400	133	153	5560	4285	1227	946	140°	7.66	0.88	0.550	0.29	6.70	Bearing Loads - Ref. 6
9. Napier Lion (1925)	492	2000	133	148	9191	4931	1273	683	170°	5.57 (castor)	0.96	0.483	0.21	8.10	Bearing Loads - Ref. 4
10. Hispano-Suiza 300 (1918)	324	1800	126	145	8034	4368	1545	840	130°	8.45	0.90	0.536	0.19	6.50	Bearing Loads - Ref. 6
11. Curtiss K-12 (1920)	420	2250	129	148	4900	3590	1036	759	130°	8.45	0.90	0.742	0.22	7.30	Bearing Loads - Ref. 6
12. Liberty-12 (1918)	420	1700	119	136	5440	3900	1046	750	130°	8.45	0.90	0.567	0.20	7.10	Bearing Loads - Ref. 6
13. Rolls-Royce Eagle (1922)	354	1800	126	143	5000	2642	1185	626	130°	13.73	0.96	1.170	0.14	7.30	Bearing Loads - Ref. 6
14. Maybach (1918)	294	1400	118	136	11736	3654	1696	528	153°	5.81	0.91	0.456	0.20	7.80	Bearing Loads - Ref. 4
15. Austro-Daimler (1918)	200	1400	123	143	7546	1926	1503	384	120°	13.40	0.92	1.450	0.10	7.40	Bearing Loads by Author using standard method

Table 4. Radial Engine Ratings and Bearing Loads

Engine (year of rating)	Brake Horsepower BHP	Engine Speed N (RPM)	Brake Mean Effective Pressure BMEP (psi)	Indicated Mean Effective Pressure IMEP (psi)	Maximum Bearing Load W (lb)	Mean Bearing Load $\bar{W}$ (lb)	Maximum Bearing Pressure p (psi)	Mean Bearing Pressure $\bar{p}$ (psi)	Oil Temperature T_{oil} (°F)	Oil Viscosity μ (lb-sec/in² x 10^{6})	Oil Specific Gravity ρ (g/cm³)	Sommerfeld Number S	Eccentricity Ratio n	Minimum Oil Film Thickness h_{min} (in x 10^{4})	Remarks
1. Wright R-1820 (1951)	1475	2800	229	286	49356	41845	4887	4143	185	4.86	0.86	0.027	0.87	3.2	Bearing Loads - Ref. 1
2. Pratt & Whitney R-2800 (1951)	2200	2800	222	278	42280	35846	3948	3347	185	4.74	0.86	0.032	0.86	3.5	Bearing Loads - Ref. 1
3. Wright R-3350 (1951)	2800	2900	228	286	48283	40450	4397	3684	185	4.74	0.86	0.031	0.88	3.0	Bearing Loads - Ref. 1
4. Pratt & Whitney R-1830 (1951)	1200	2700	192	237	27243	22153	2865	2329	185	4.74	0.86	0.045	0.76	4.49	Bearing Loads - Ref. 1
5. Wright R-2600 (1947)	1900	2800	206	256	38416	31213	3830	3112	170	6.52	0.86	0.048	0.84	4.1	Bearing Loads - Ref. 1
6. Armstrong-Siddeley Jaguar V (1925)	388	1700	120	128	6508	5700	685	600	140	11.14 (castor)	0.96	0.258	0.30	13.0	Bearing Loads - Ref. 5
7. Bristol Jupiter IV (1926)	425	1600	120	131	10638	8684	1271	1038	140	11.14 (castor)	0.96	0.140	0.46	8.2	Bearing Loads - Ref. 5
8. Wright R-1750 (1929)	525	1900	125	139	17428	15193	1505	1312	140	12.70	0.88	0.150	0.43	13.0	Bearing Loads - Ref. 4
9. Bristol Jupiter VIII (1928)	440	2000	99.4	115	14000	11200	2000	1600	140	11.14 (castor)	0.96	0.114	0.52	7.7	Bearing Loads - Ref. 5
10. Armstrong-Siddeley Tiger I (1932)	580	2000	115	130	17301 14211	13754 11593	1662 1365	1321 1114	150	7.82	0.87	0.115 ?	0.52 ?	10.0 ?	See "Bearing Load Analysis - Radial Engines" Section
11. Armstrong-Siddeley Panther III (1931)	500	2000	119	133	10914	8473	1185	920	150	7.82	0.87	0.139	0.45	11.0	Bearing Loads - Ref. 5
12. Wright Fictional "R-1416" See Table 6.		2800		286	42489	34334									Fictional 7-Cylinder R-1820 for Bearing Load Comparison
13. Bristol Jupiter VI (1928)	486	1870	117	130	15530 11969	12403 9572	2164 1668	1728 1325	150	8.63 (castor)	0.96	0.099	0.55	7.2	See note for Engine 10
14. Pratt & Whitney R-1340 (1926)	450	2100	126	141	15222	13169	1718	1486	140	18.70	0.88	0.147	0.45	10.0	Bearing Loads - Ref. 4
15. Pratt & Whitney R-1860 (1934)	567	1950	124	141	20844	18460	2071	1835	140	18.70	0.88	0.110	0.53	9.8	Bearing Loads - Ref. 4
16. Bristol Pegasus XX (1937)	878	2475	160												Data Unavailable to Author
17. Bristol Hercules (ca 1958)	2300	2900	266												Data Unavailable to Author
18. Bristol Centaurus 661 (1951)	2625	2800	227	285	47397	39482	3920	3266	185	4.74	0.86	0.033	0.87	3.5	Bearing Loads by Author, Figs. 19 & 20

take-off rating of the engine and may not represent the actual maximum load encountered in service. The silver-lead-indium bearing was developed by Pratt & Whitney for the R-1830, which, according to Figure 5, should have been quite happy with a copper-lead bearing. Reference 21 indicates that the bearing was failing in an over speed situation in military applications. I would like to emphasize that this representation should be taken as an indication of how maximum bearing loads evolved and not as an indication of the likelihood of an engine bearing failure.

Engine designers did use the maximum unit pressure as a design guide in the time frame we are considering here and they also used the "PV" or rubbing factor that was supposed to be an indicator of the maximum bearing temperature. It was defined as the mean unit bearing pressure multiplied by the peripheral journal speed, which gives it the units of ft-lb/in²/sec. Shaw and Macks (1) have shown the rubbing factor to be relatively meaningless as a measure of the thermal loading on a bearing so I have not included it in this analysis. They have presented a more rigorous technique for evaluating temperature limited operation but insufficient data for the engines under consideration here make this type of evaluation impractical.

Figure 5 makes it clear that most engines prior to 1930 had maximum power ratings that resulted in bearing pressures beyond the fatigue strength of tin based Babbitt. Here again the Curtiss V-1570 stands out as being well outside the range of the other in-line and V engines. You will recall from Figure 2 that its crankpin diameter and effective bearing length relative to its bore were significantly less than other engines of that period and that is reflected here in high bearing pressures. It appears from the record that the V-1570 had significant bearing problems through most of its life.

C. F. Taylor (29) reported in March, 1927 in a visit, presumably as a consultant, to the Curtiss Co. that a GV-1550 engine was equipped with steel backed Babbitt bearings. Later Memorandum Reports from the Material Division at Wright Field indicate that in 1929 the main and master rod bearings were not "capable of sustained full throttle operation at 2,400 rpm". Copper-lead bearings were apparently introduced in 1929 but problems continued. A report from 1934 deemed a test successful after observing average crankpin bearing wear of 0.0012" in ten hours of operation and two bearings that had "commenced to flow slightly" and a third that was "slightly burned".

The Curtiss D-12 was operating with Babbitt bearings in this period and could apparently withstand over-speeds to 3,500 rpm in power dives without significant bearing distress. Prescott and Poole (4) have estimated the bearing pressure at 1,837 psi under those conditions, which is still below the V-1570 value of Figure 5.

It is interesting that here again the Armstrong-Siddeley Jaguar was in about the right place for the time.

Mean Unit Bearing Pressures

The mean unit bearing pressures influence the other variable that is of interest, i.e. the minimum oil film thickness at which the bearing loses the ability to support its load hydrodynamically and friction increases rapidly. The measure of this phenomenon is the Sommerfeld number (S_o). The typical relationship between a bearing's coefficient of friction and S_o is shown in Figure 6. The S_o is a bearing's equivalent to the Reynolds number. The parameters in the Sommerfeld number are defined in Figure 27. It should be noted that it varies inversely with the mean unit pressure and directly with journal speed and the lubricating oil viscosity. Referring to Figure 6, as the speed decreases and/or the mean unit bearing pressure increases the S_o number reaches a point where the friction coefficient begins to increase rather than decrease. When this occurs more heat is generated and the temperature of the lube oil increases causing its viscosity to decrease, which pushes the S_o even further to the left (Fig. 6), increasing the friction even more until the bearing fails or the oil supply is increased.

Tables 3 and 4 show the values of oil temperature and viscosity used to calculate the Sommerfeld Number. References 25, 26, 27 and 28 were the primary sources for these numbers. In general, the oil temperature to the bearings follows a straight line trend from about 120° F in 1918 to 185° F in

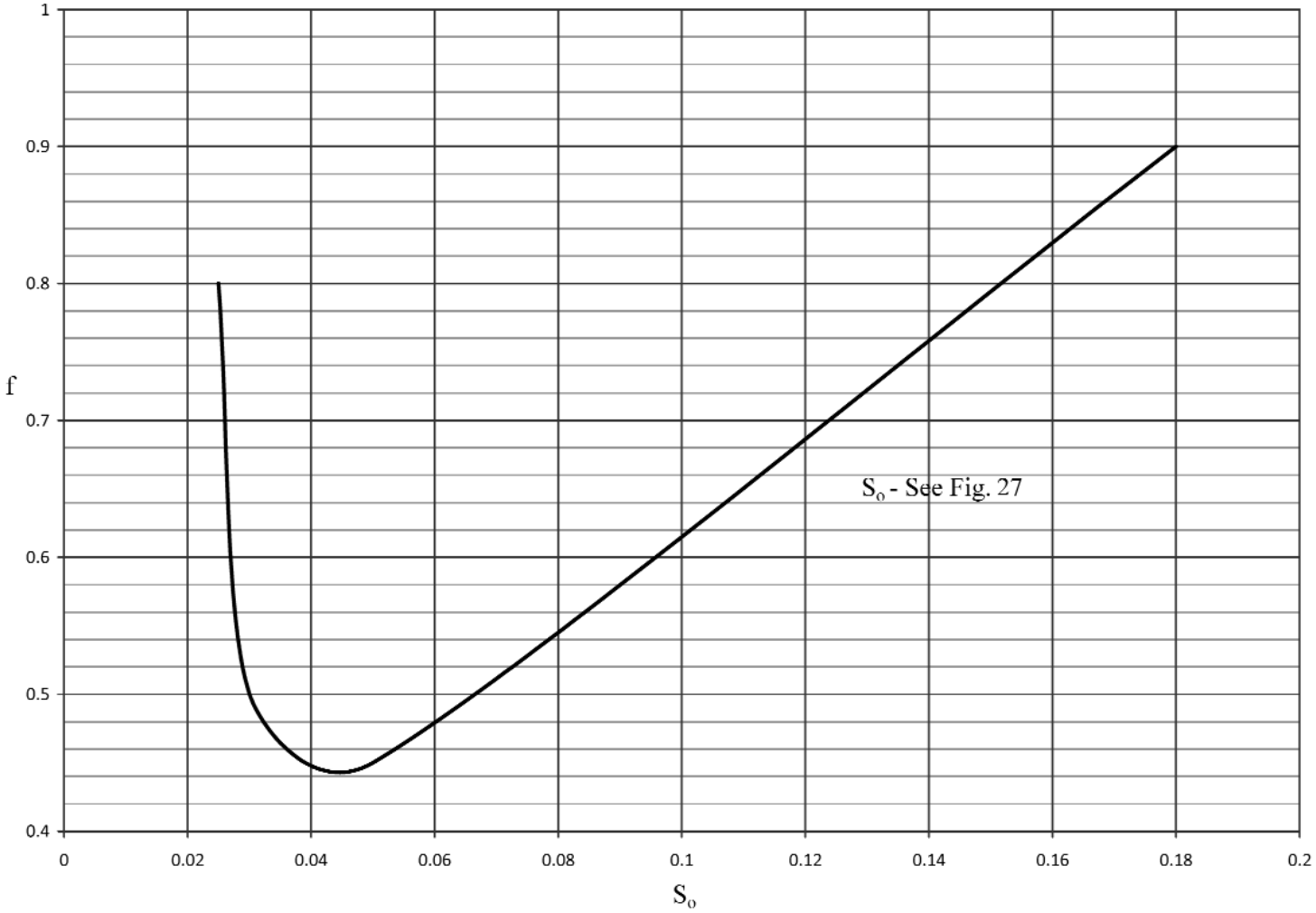

Figure 6 Journal Bearing Friction Coefficient versus Sommerfeld Number

1955. Castor oil is used where appropriate and is noted in the tables. Its viscosity is in the vicinity of an SAE 40. Later U.S.A. oils were in the SAE 50-60 range as were the later Bristol specifications.

The value of S_o at which the transition from hydrodynamic lubrication to partial film lubrication occurs is a function of the bearing material and the detailed design of the bearing. In general, any interruptions in the bearing surface where there are high oil film pressures will cause the transition point to move to the right in Figure 6. Grooves allow higher oil flow at the expense of lower bearing load capacity. If grooves are used to increase oil flow they should be axial rather than circumferential and should be in a lightly loaded area in the journal (more on this in Crankpin Bearing Lubrication section). With regard to the effect of bearing material, Reference 1 gives minimum values of S_o for tin-base Babbitt at 0.050, copper-lead at 0.009 and silver-lead-indium at 0.005.

Figure 7 shows how the Sommerfeld Number changed with time for various in-line and radial engines. Note that the lowest values in the 1950-55 era are well above the limits given above with the possible exception of tin based Babbitt, which indicates that the early bearing failures must have been primarily fatigue failures, wear due to misalignment, and inadequate lubrication rather than an inadequate Sommerfeld number.

The eccentricity ratio is defined in Figure 8. In order to calculate an eccentricity ratio for an engine crankpin bearing I am making the assumption that the mean load is controlling and that a reasonable value can be obtained by using test results for bearings with constant loads, in this case from NACA work at Cornell University (24). I have compared this approach with the results of an analysis that utilized the actual dynamic loading for the Wright R-1820 engine at 2,500 rpm and 245 psi imep. The value obtained for eccentricity ratio was 0.88 (Burwell, reported in (1)). With my approach the value obtained was 0.86. Since we are looking at trends over time, I have concluded that this approach is justified.

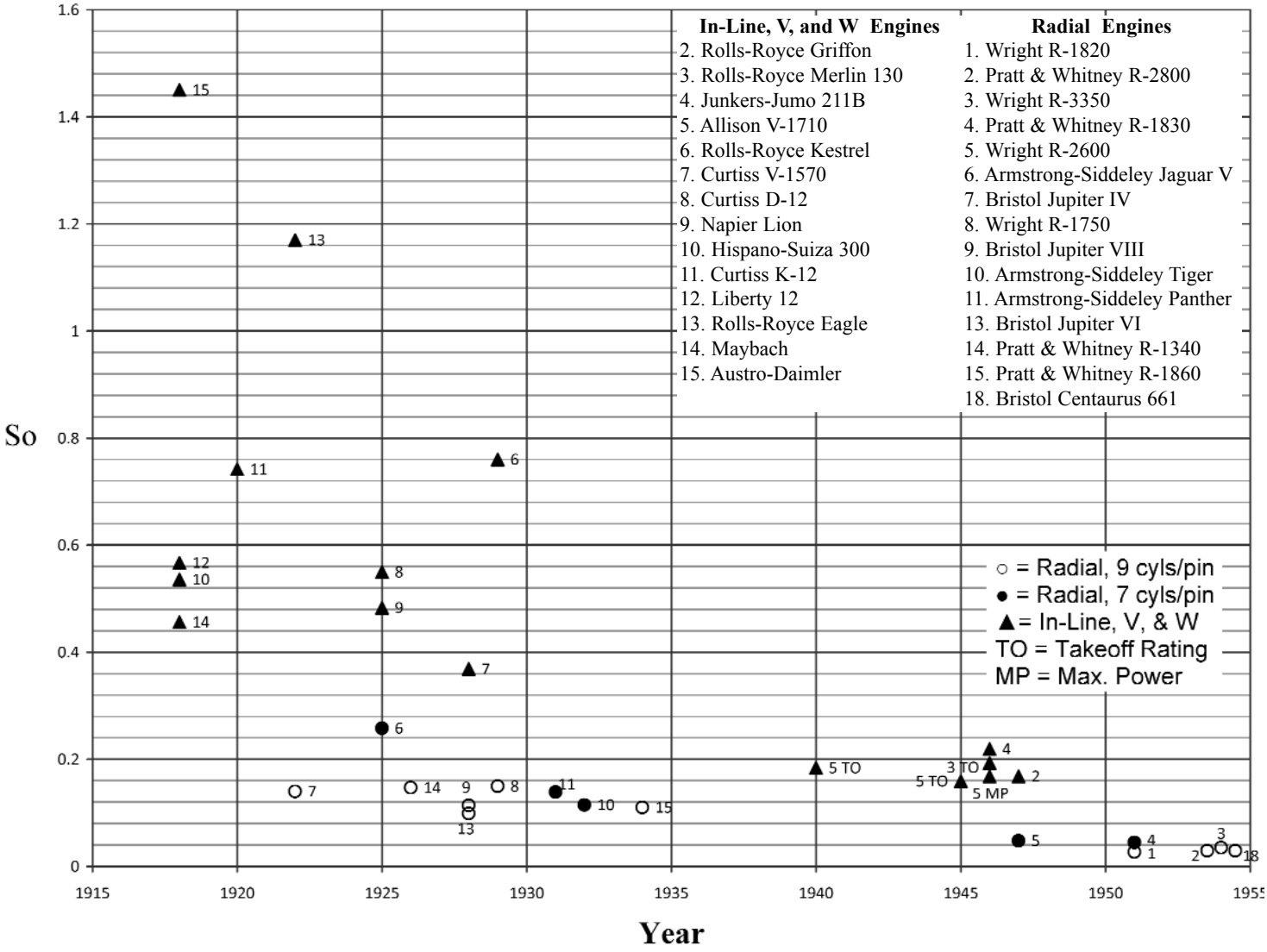

Figure 7: Sommerfeld Number versus Time, Various Engines

The relationship between the eccentricity ratio and the minimum film thickness is shown on Figure 8 and the minimum film thickness versus time for the engines is shown in Figure 9. It should be noted that, due to a lack of data on bearing clearances, I have assumed a constant ratio of bearing diameter to diametral clearance as given on Figure 27.

Comparing Figures 5 and 7 we see that, while the maximum unit bearing pressures are in the same range for the in-line V and radial engines (4,000 ~ 5,000 psi), the Sommerfeld numbers are lower for the radial engines by a factor of 4 or 5. This is because the mean unit bearing pressures are much higher for the radial engines (see Tables 3 and 4), and I have assumed significantly higher bearing clearances for the radial engines. If the clearance assumption were the same for the in-line V and radial engines the Sommerfeld number would still be half the value of that of the in-line Vs or the radials.

It is probably safe to say that the radial engine was pushing bearing technology harder than the in-line V engines from WWII to the end of the era.

Bearing Load Evaluation

Assumptions

In order to calculate bearing loads one must have the pressure and inertia loads as a function of crankshaft angle. This requires knowing the rotating and reciprocating weights of the moving parts and constructing a pressure-crank angle diagram for the speed and power condition being evaluated. This technique was well established and will not be repeated here in any great detail. The assumptions generally made are as follows:

The imep used to construct the P-V diagram is usually assumed to be 90% of the fuel-air cycle value. The actual peak firing pressure is assumed to be 75% of the fuel-air cycle firing pressure and occurs at 20° after top dead center. It should be noted that the bearing loads given in this paper are from a wide variety of sources over a broad time period. The methods of developing a fuel-air cycle have varied over the time period under consideration here but I have found remarkably good agreement when I have checked my approach against older data. The bearing loads reported in the literature do not usually give the imep, only the brake horsepower and speed and so I have had to estimate the imep using engine friction data and supercharger performance where applicable. I have used Reference 30 to construct fuel-air cycles.

With regard to the kinematics and dynamics of the connecting rods, the effects of the articulated motion on the inertia loading is usually ignored and assumed to behave like a normal rod attached to the crankpin. The pressure

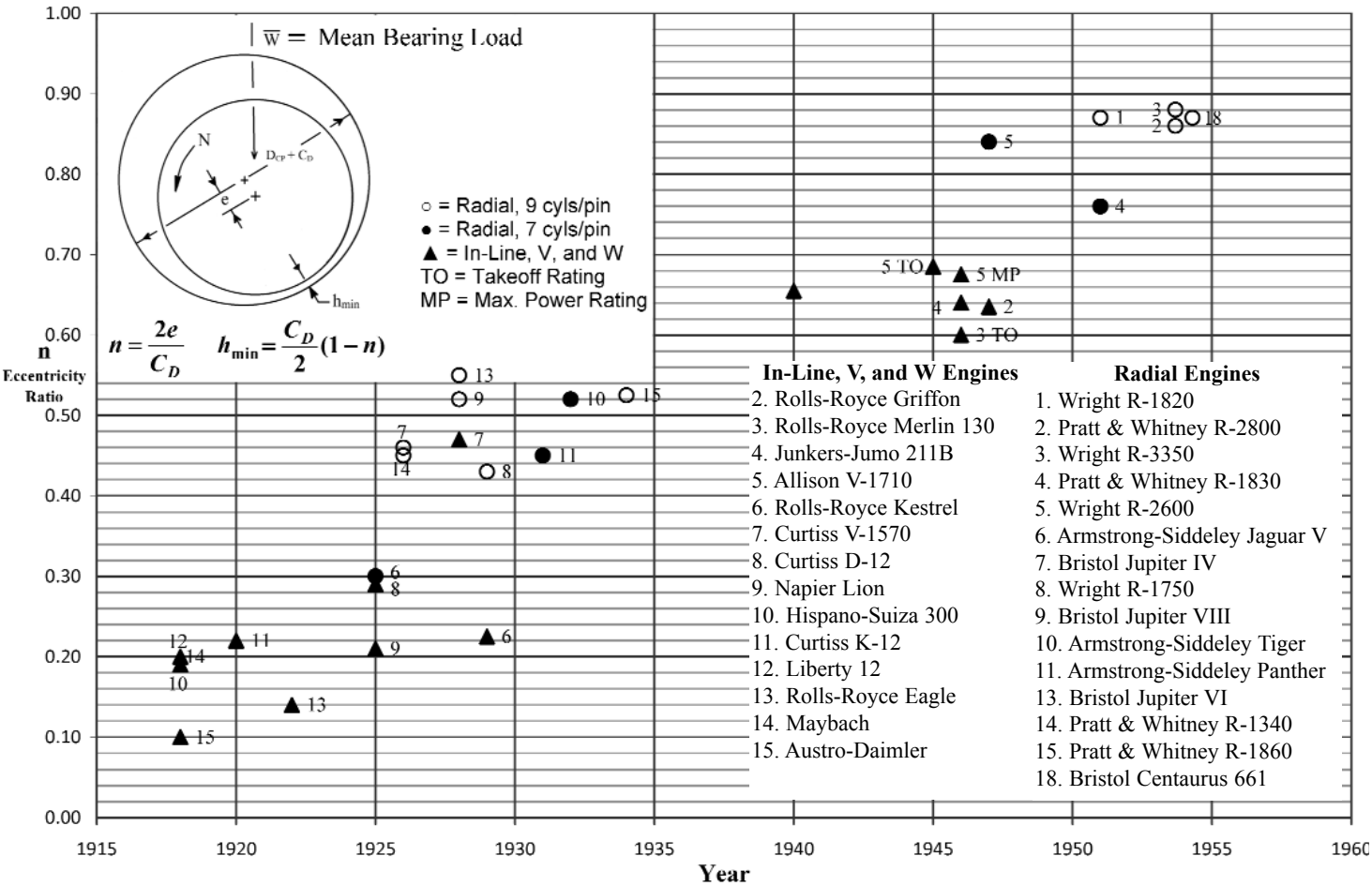

Figure 8. Crankpin Journal Eccentricity Ratio versus Time, Various Engines

load on articulated rods is assumed to act on the crankpin directly. The in-line connecting rod, master rod and articulated rods are treated as two masses, one reciprocating and one rotating rather than as a solid body with a moment of inertia. Reference 1 looks at these assumptions and shows that they are justified.

Bearing Load Analysis- In-line Engines

The use of dimensional analysis to generalize the applicability of bearing analyses appears to have been initiated at the NACA and is summarized in (1). The usual dimensionless groups are formed with the result that, for a specific engine, the bearing load can be represented by

W/imep = function of (N^2/imep, crank angle)
(see Tables1-4 for nomenclature)

Allison V-1710 analysis results using this expression are shown in Figure 10. The maximum load is seen to occur at crank angles of 20°, 120°, and 680°, depending on the value of N^2/imep. In the 20° portion pressure forces dominate while in the 120° portion both inertia and pressure forces are in play and at 680° inertia forces are controlling. Thus, with this approach an entire map can be generated with relatively few calculations.

Such a map showing imep versus engine speed is shown in Figure 11. Lines of constant bearing load and constant indicated horsepower are shown. To minimize the maximum bearing load at, for example, 1,800 indicated horsepower, one would operate the engine at about 3,000 rpm and an imep of 280 psi.

The dimensional analysis approach also works for the mean bearing load; Allison engine results are shown in Figure 12. Results for the entire engine operating range were obtained by analyzing seven conditions, but two would have sufficed since the result is a straight line.

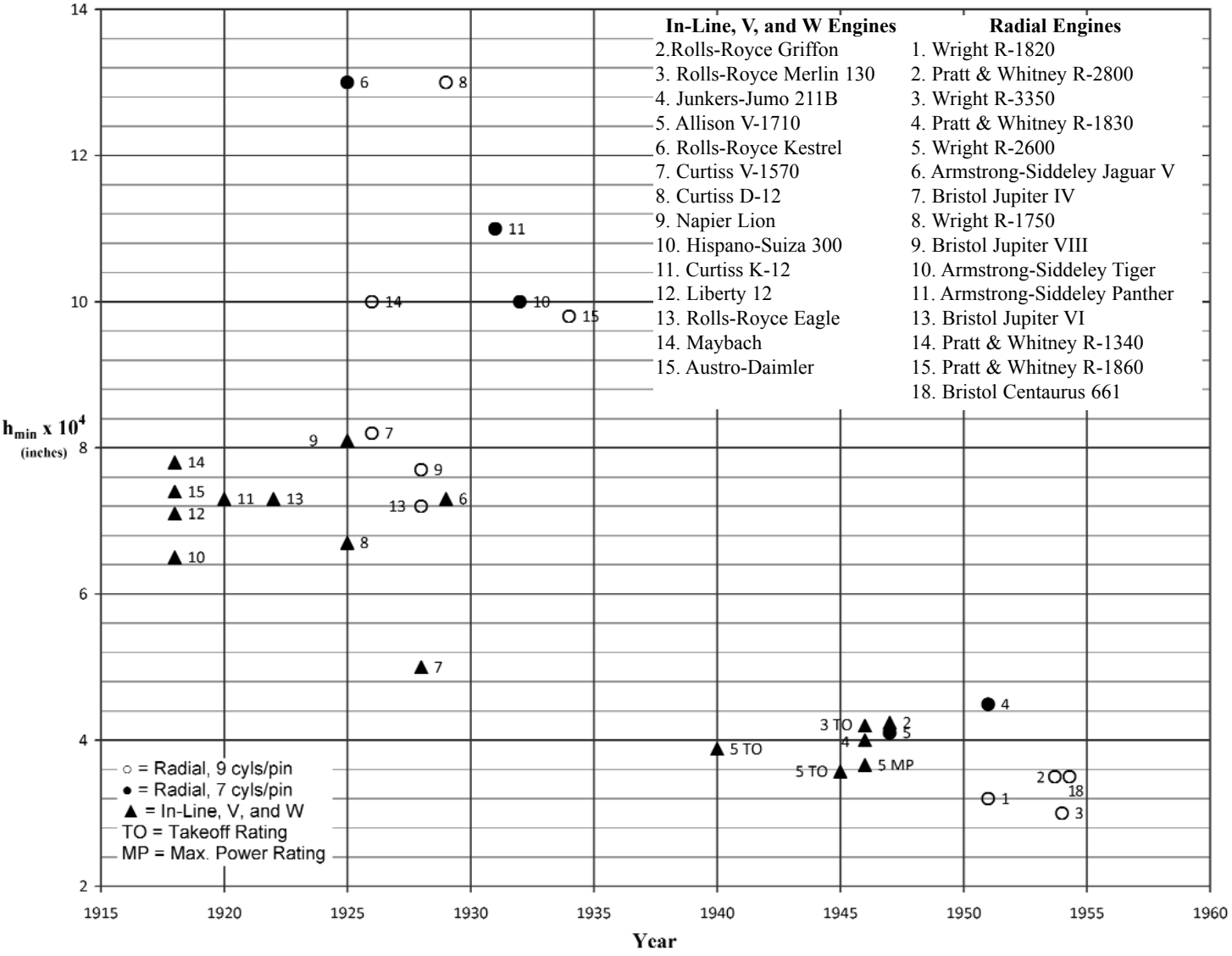

Figure 9. Minimum Bearing Oil Film Thickness versus Time, Various Engines

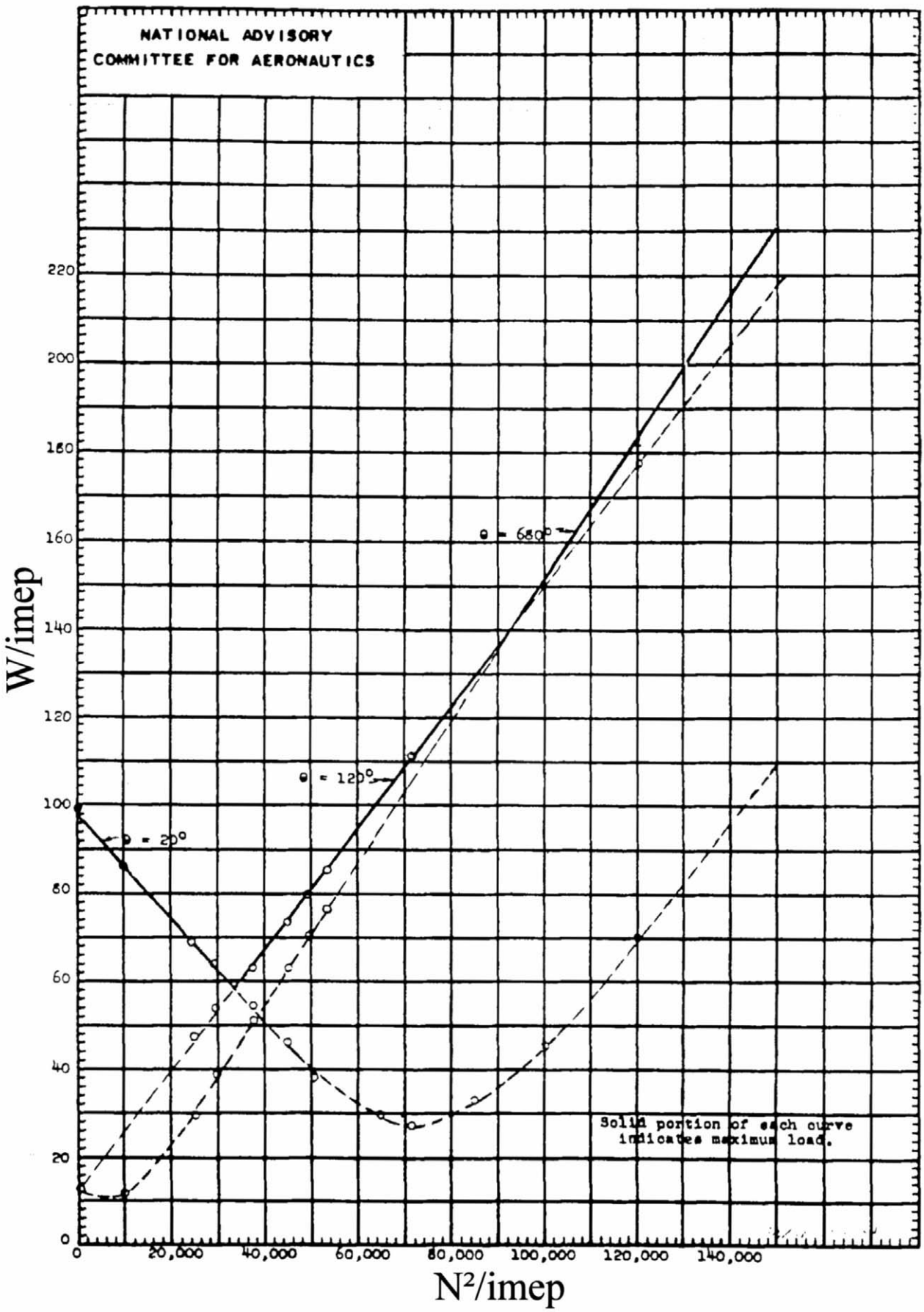

Figure 10. Maximum Bearing Load (W/imep) versus Engine Speed (N2/imep), Allison V-1710

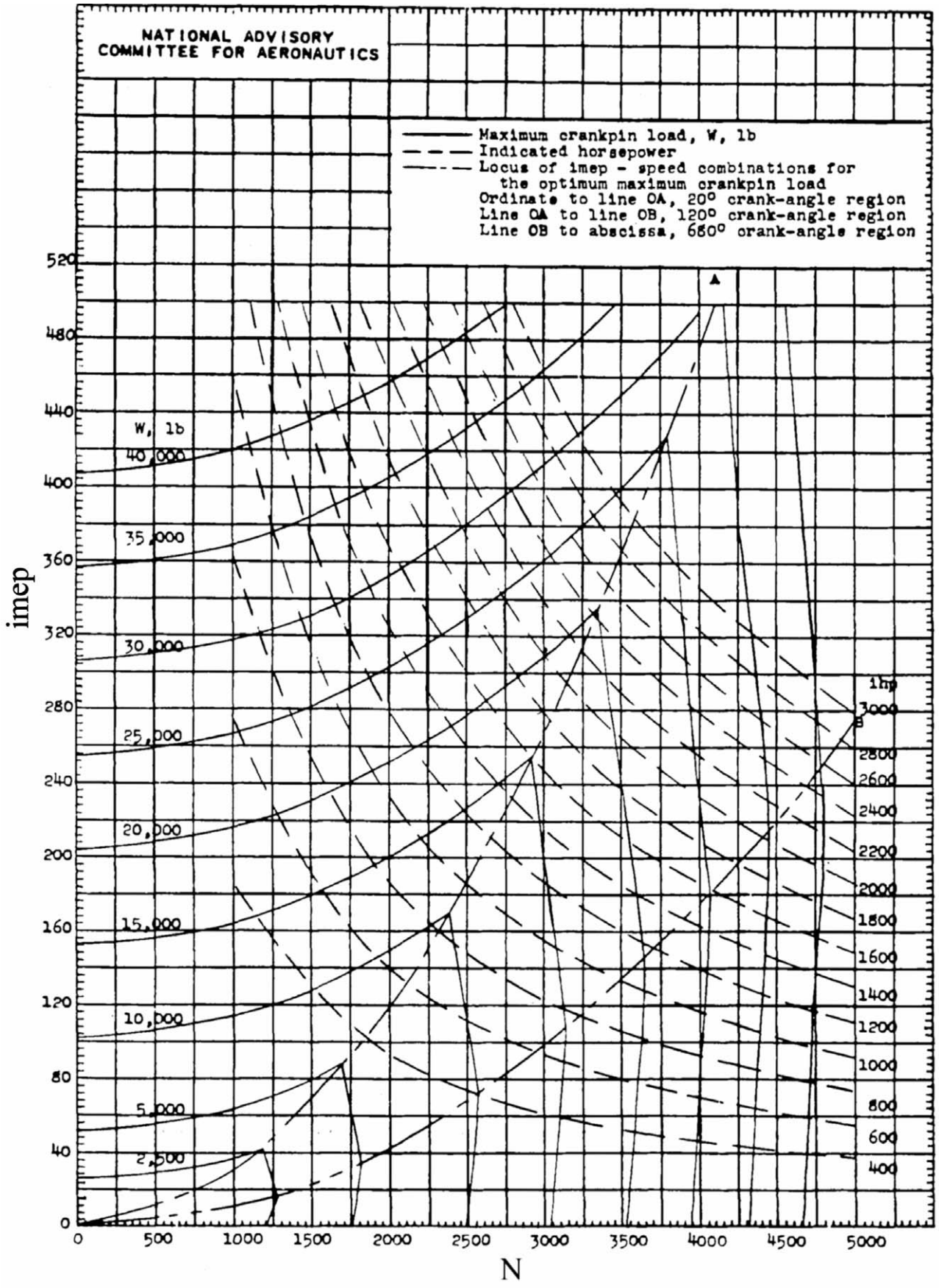

Figure 11. Indicated Mean Effective Pressure versus Engine Speed with Lines of Constant Maximum Bearing Load and Indicated Horsepower, Allison V-1710

This is an excellent demonstration of the power of dimensional analysis, which one hopes will not be lost to engineers in the era of high speed computers.

Prescott and Poole (4) attempted to formulate a method for evaluating crankpin bearing loads using empirically derived constants. For the mean bearing inertia load they defined an effective weight that was equal to the rotating weight at the crankpin plus a constant, K , multiplied by the reciprocating weight (this is the effective weight I have used in Figure 4). They defined similar constants to be multiplied by the piston area and bmep to arrive at the gas pressure component and maximum crankpin force. In their later work, Shaw and Macks (1) found this kind of approach to be less than satisfactory because "no simple approach has been found by which a change in the magnitude of the reciprocating and rotating weights may be taken into consideration by dimensional analysis".

I have attempted to generalize the in-line engine bearing loads by combining the approaches of Prescott and Poole with the dimensional analysis technique as defined by Shaw and Macks. Figure 13 shows a dimensionless mean bearing load (defined on Figure 27) plotted against a dimensionless mean inertia load. The resulting linearity of this plot seems to justify this approach, at least with regard to the mean bearing load. Given the wide variety of the sources and engine geometries, I was quite surprised by this result. The reader will note that I have used the same expression as Prescott and Poole to define the equivalent mass to give the mean inertia load. Figure 14 shows how the constant, K, was arrived at for the various engines. K is plotted versus the ratio of reciprocating to rotating weights. The solid line applies to one reciprocating mass per crankpin and shows good agreement with the three engines for which I calculated the result. I also made the calculation for a hypothetical opposed piston engine with the same weight ratio as the Allison V-1710 and found that, as one would expect, it gave a similar result as one reciprocating weight per crankpin. I am not certain why there is a significant difference between the K values for the Liberty 12 and the Curtiss V-1570, and the four very different engines with K values of 0.54. The weight ratio is somewhat less for those two engines and perhaps the K value starts to approach the one weight per

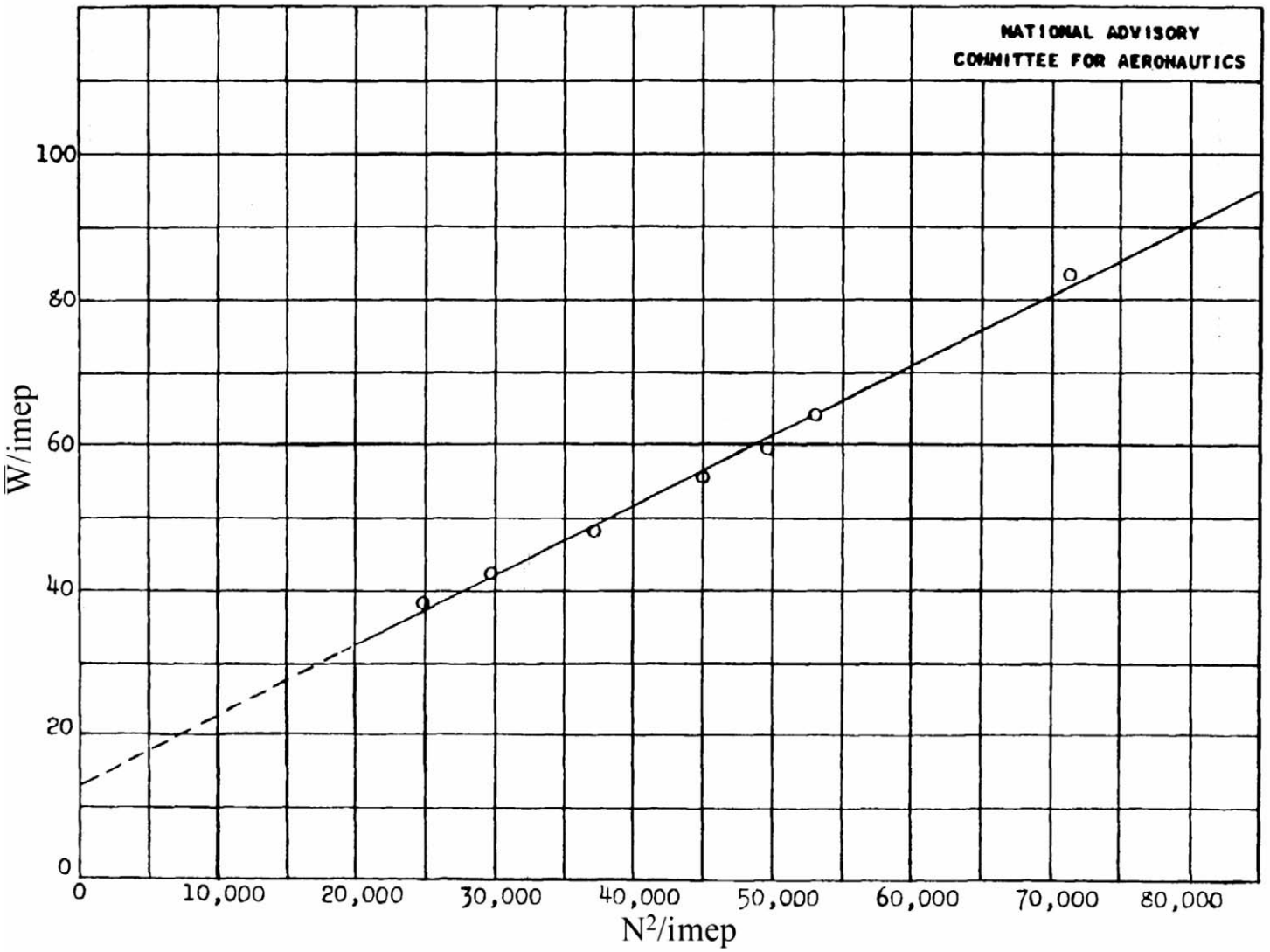

Figure 12. Mean Bearing Load ($\overline{W}$/imep) versus Engine Speed (N^2/imep)

crankpin result as its value approaches one. It will be recalled that the Maybach engine had cast iron pistons and that is the reason for its position on the far right of the curve in Figure 14.

The two Figures, 13 and 14, make it possible to estimate the mean bearing load for any in-line engine if the weights and imep are known. I have used this approach to get the loads for the Merlin 130, the Junkers Jumo 211B and the Rolls-Royce Griffon as shown in Table 3. The maximum load for any in-line engine is fairly easy to calculate since, as Figure 10 shows, the peak load occurs at either 20° or 120° after top dead center of the leading cylinder in the direction of rotation for 60° bank angles (135° for 45° bank angle).

A dimensionless maximum bearing load for in-line engines is shown in Figure 15. Here the spread in the results is significantly greater than for the mean loads of Figure 13. The reasons for this are as follows:

The compression ratios of these engines are different and while the compression ratio has a minimal effect on mean bearing load, it does have a strong influence on the maximum load.

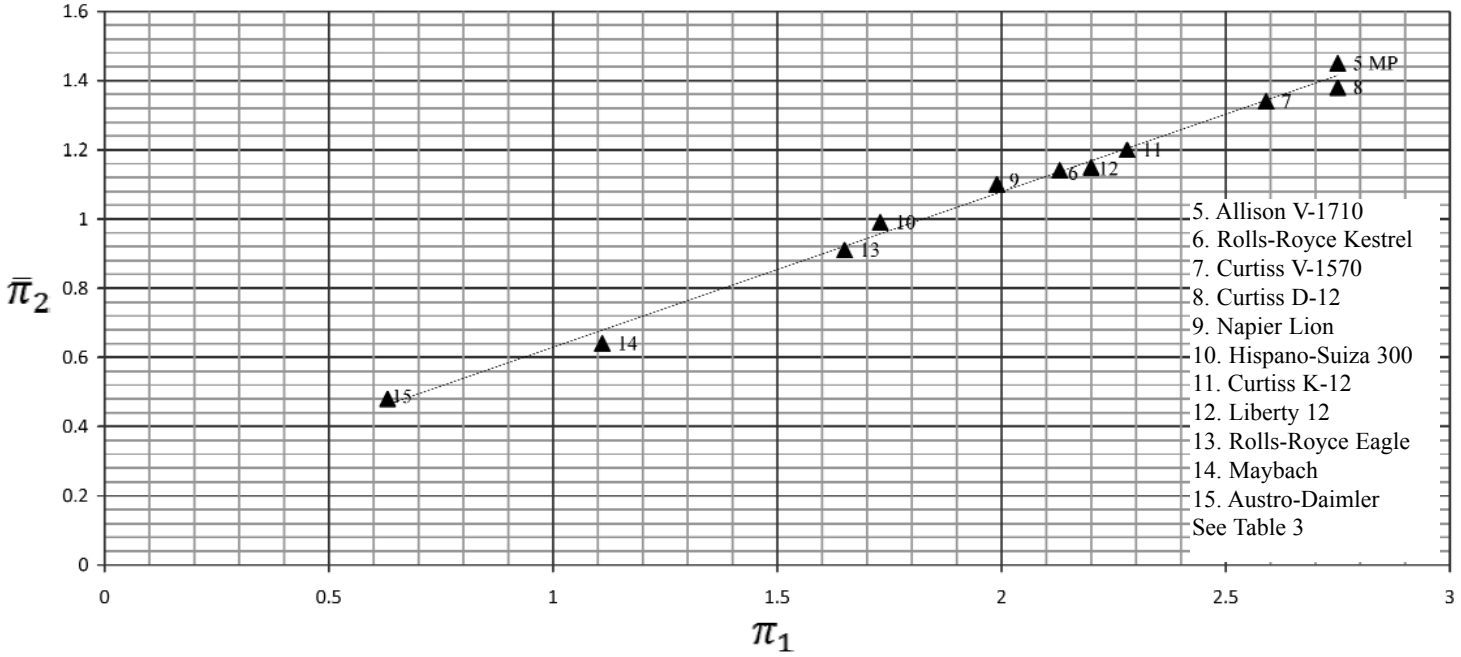

Figure 13. Dimensionless Mean Crankpin Bearing Load versus Dimensionless Mean Inertia Load, In-Line, V, and W Engines

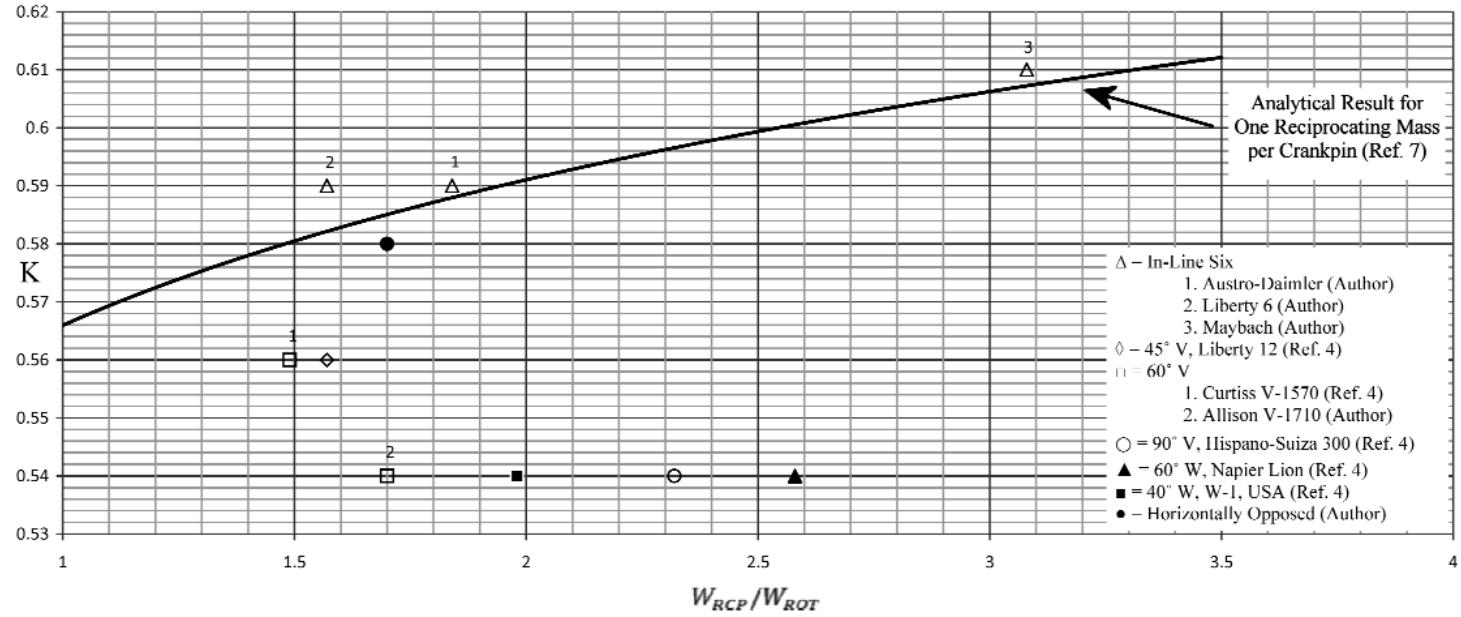

Figure 14. K, the Constant for Evaluating the Effective Mass per Crankpin to Give the Mean Inertia Load versus the Ratio of Reciprocating to Rotating Weight per Crankpin

Since the data in Figure 15 come from many sources over a wide time span, there may be significant differences in assumptions about peak firing pressures and cylinder pressure at 120° after top center.

I calculated the maximum loads for engines 2, 3, 4, 5, and 15 and there is much less scatter if one draws a straight line through these four points.

An alternate way of showing the maximum bearing pressure is given in Figure 16. Here the maximum load is shown in the ordinate as a ratio of dimensionless maximum to mean bearing load versus the dimensionless mean inertia load. I have also shown a dashed curve representing the results for the Allison V-1710 from (10). Here again the compression ratio effect is evident. The only engine with a higher compression ratio than the Allison is the Jumo at 7:1 (see Table 1 for the compression ratios), and it falls on the Allison line. The Rolls-Royce Merlin, Kestrel and Griffon all had compression ratios of 6:1, and both fall on or near a parallel curve, which is a best fit for the data.

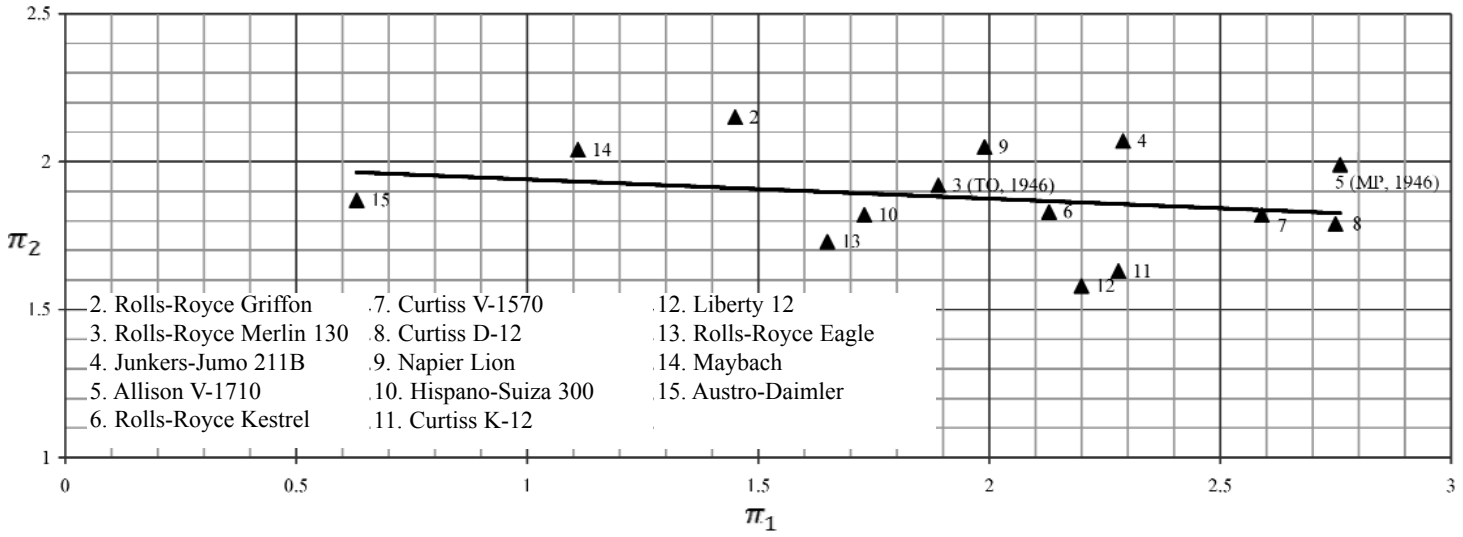

Figure 15. Dimensionless Maximum Crank Pin Bearing Load versus Dimensionless Mean Inertia Load, In-Line, V, and W Engines

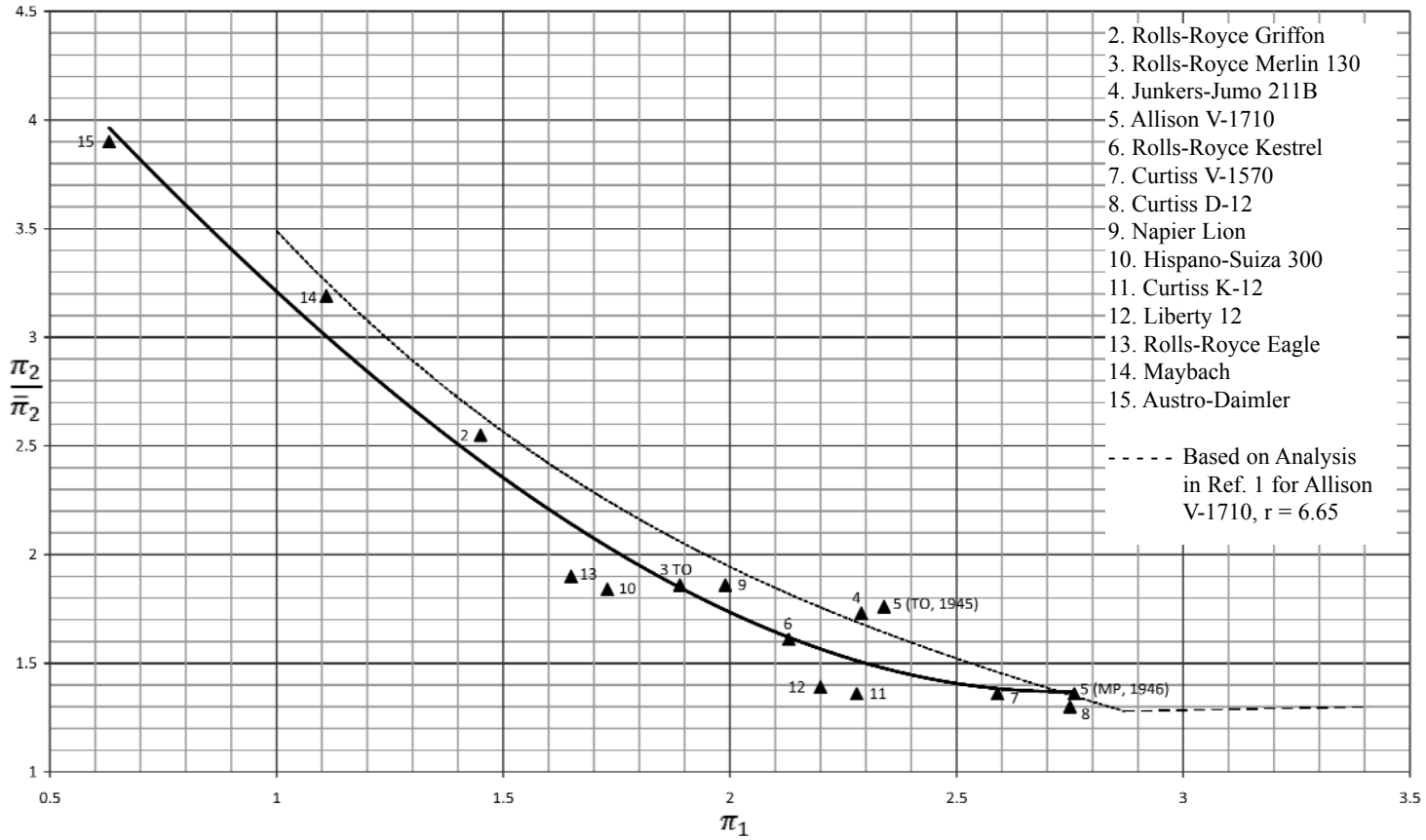

Figure 16. Ratio of Maximum to Mean Crankpin Bearing Load versus Dimensionless Mean Inertia Load, In-Line, V, and W Engines

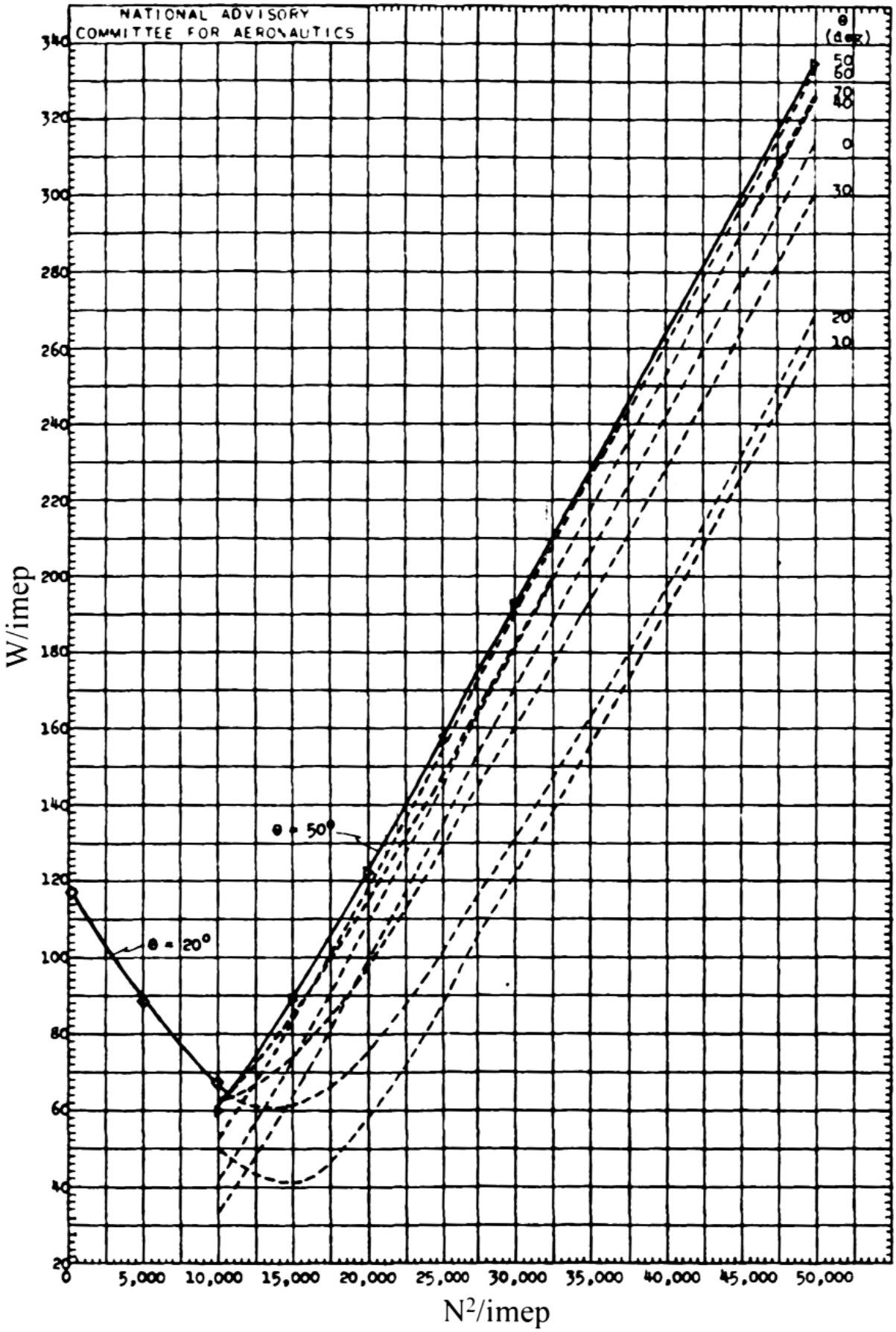

Figure 17. Maximum Bearing Load (W/imep) versus Engine Speed (N²/imep), Wright R-1820

Bearing Load Analysis- Radial Engines

With the radial engines I have followed the method of Shaw and Macks as described in Reference 11. Again, dimensional analysis is used and the same groups are used as were used for in-line engines. The result for nine cylinders per row is shown in Figure 17. The peak bearing load occurs at either a 20° or 50° crank angle.

A relationship exists for the radial engine that simplifies the analysis required to get the magnitude and direction of the crankpin bearing load. The following expression was first presented by Prescott and Poole (4) without derivation.

$$W_i = 28.4x10^{-6}\frac{L}{2N^2}\left[W_{ROT} + \left(\frac{1}{2} + \frac{1}{4}\left(\frac{L}{2l_{CR}}\right)^2\right)W_{RCP}\right]$$

Shaw and Macks verified its accuracy for five, seven, and nine cylinders; it does not work for three cylinder radials.

This equation represents the resultant inertia force vector from all of the rotating and reciprocating inertias and acts along the crank axis and rotates with it. The portion of this equation that involves the two masses, reciprocating and rotating, gives the effective mass, M_e, that results in the mean inertia load.

Figure 18 is a polar diagram for the Wright R-1820 at 2,500 rpm and 245 psi imep. The outer circle in Figure 18 is the resultant inertia force given by the equation above. The inner circle is the rotating inertia only, represented by the vector OA at a 20° crank angle. The vectors labeled 1-9 are the resultant gas and inertia vectors for the nine cylinders and, when added to OA, give the resultant bearing load vector OD. The calculation is simplified if the total inertia vector OB is added to the individual cylinder pressure loads only, giving the vector OC in Figure 18. When this vector is moved to a parallel position with its tail connected to the head of OB it results in the same final vector, OD. Note that only about 80° of crank angle need be analyzed because the load pattern repeats itself beyond that interval. Figure 20 gives the resultant load direction relative to the engine axis but this can be changed by a suitable transformation of coordinates to give the magnitude and direction relative to the crank axis or the master rod axis, depending on what you are trying to do. Caution is required in interpreting Figure 18 because the crank angle is noted on the load curves and not on the outer diameter of the inertia circle. Thus the peak load occurs at 50°, 130° etc. The angles given on the outer circle refer to the direction of the load vector with respect to the engine axis.

The existence of the expression for the total inertia force given above makes possible a simpler presentation of the results since the dimensional analysis approach makes the solution valid for all radial engines with nine cylinders per row. By confining their results to the not really dimensionless N^2/imep, Shaw and Macks have made the evaluation of the effect of changes in dimensions and weights unnecessarily complicated. If N^2/imep is made truly dimensionless by using the inertia force from the above equation and dividing it by the bore squared and imep, a simple single line is generated that applies to all nine cylinder per row engines with a compression ratio of 6.7:1.

Figure 19 shows such a plot together with a similar plot for seven cylinders per crankpin based on a similar analysis by Shaw and Macks. The dimensionless groups defined in this Figure make it very simple to evaluate changes in weights, dimensions, imep and engine speed. Engines 10 and 13 in Figure 19 had bearing loads given in (5) that exceeded the resultant total inertia load, which, looking at Figure 18, is clearly impossible. By taking the resultant inertia forces for those two engines and the ratio of maximum inertia load to maximum bearing load at the equivalent condition for the R-1820, I was able to get the reasonable looking results for those two engines shown in Figures 19 & 20.

Figure 20 shows the dimensionless mean bearing load as a function of the dimensionless inertia load for both seven and nine cylinders per crankpin. In both this figure and Figure 19, the agreement between the reported numbers from a wide variety of sources and the results of the dimensional analysis is good given the same caveats as discussed under the in-line engine results. Here the differences in compression ratio show up as higher loading for the earlier engines with lower compression ratios. A glance at Figure 18 will explain this phenomenon. The firing pressure loads are counteracting the total inertia load, represented by the outer circle in Figure 18.

Results

In this section of the paper I will present some additional findings pertaining to the subject of crankpin bearings not covered in the material presented so far. I feel that the reader may have a better appreciation for some of this material after having looked over the main body of work, so rather than try to inject it at various points in the narrative I am placing it at the end, like the concert pianist who saves the flashy stuff for the encores.

Since there always is an interest in comparing and contrasting the Rolls-Royce Merlin and the Allison V-1710, I have prepared Table 5 comparing the maximum and mean crankpin bearing loads and unit pressures for these two engines. I have done this at the same operating conditions of rpm (and piston speed since the strokes are the same) and imep. The brake horsepower for the V-1710 is a little higher because of its larger displacement. At the standard compression ratios of these two engines the maximum bearing pressures are nearly the same since the crankpin dimensions of the V-1710 are larger (see Table 1). The mean bearing load of the V-1710 is higher due to its greater reciprocating and rotating weights. When the V-1710's compression ratio is reduced to 6 :1 its maximum bearing pressure is 90% of the Merlin's. Mean bearing loads are not affected by the change in compression ratio.

In order to compare the effect on the crankpin bearing loads of the number of cylinders of a radial engine I have

prepared Table 6. I have used the basic dimensions of the Wright R-1820 so the comparable 7-cylinder per row engine is an R-1416. I have made the appropriate adjustments to the reciprocating and rotating inertias assuming the crankpin dimensions stay the same. According to Table 6 one could reduce the projected crankpin bearing area of the R-1416 by about 14% to keep the same maximum bearing pressure. Such a reduction would reduce the rotating inertia and a further slight reduction in bearing area could be realized.

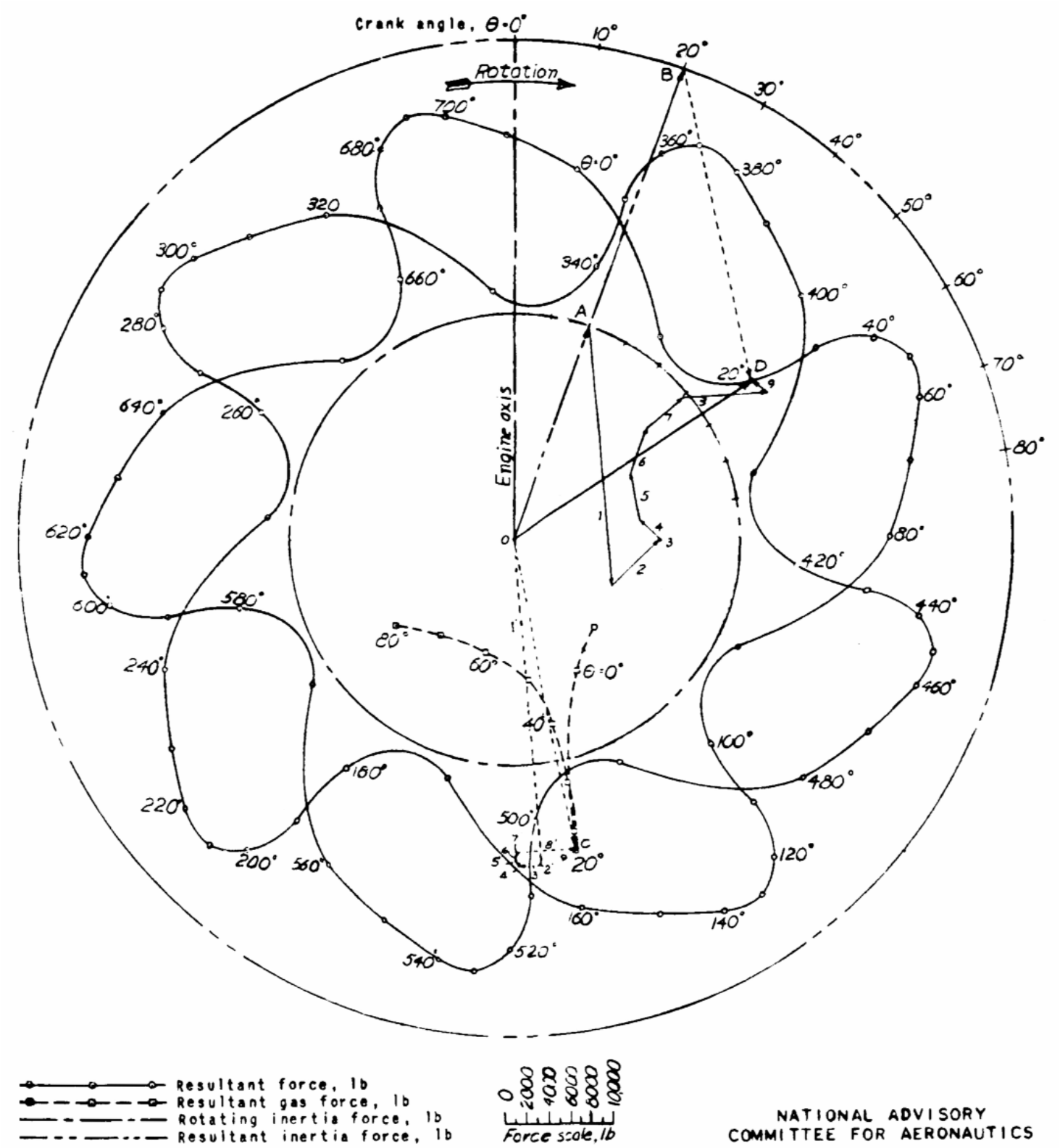

Figure 18. Polar Diagram Showing Crankpin Resultant Force Magnitude and Direction with Respect to the Engine Axis Wright R-1820: Engine Speed = 2,500 RPM; imep = 245 psi; r = 6.7

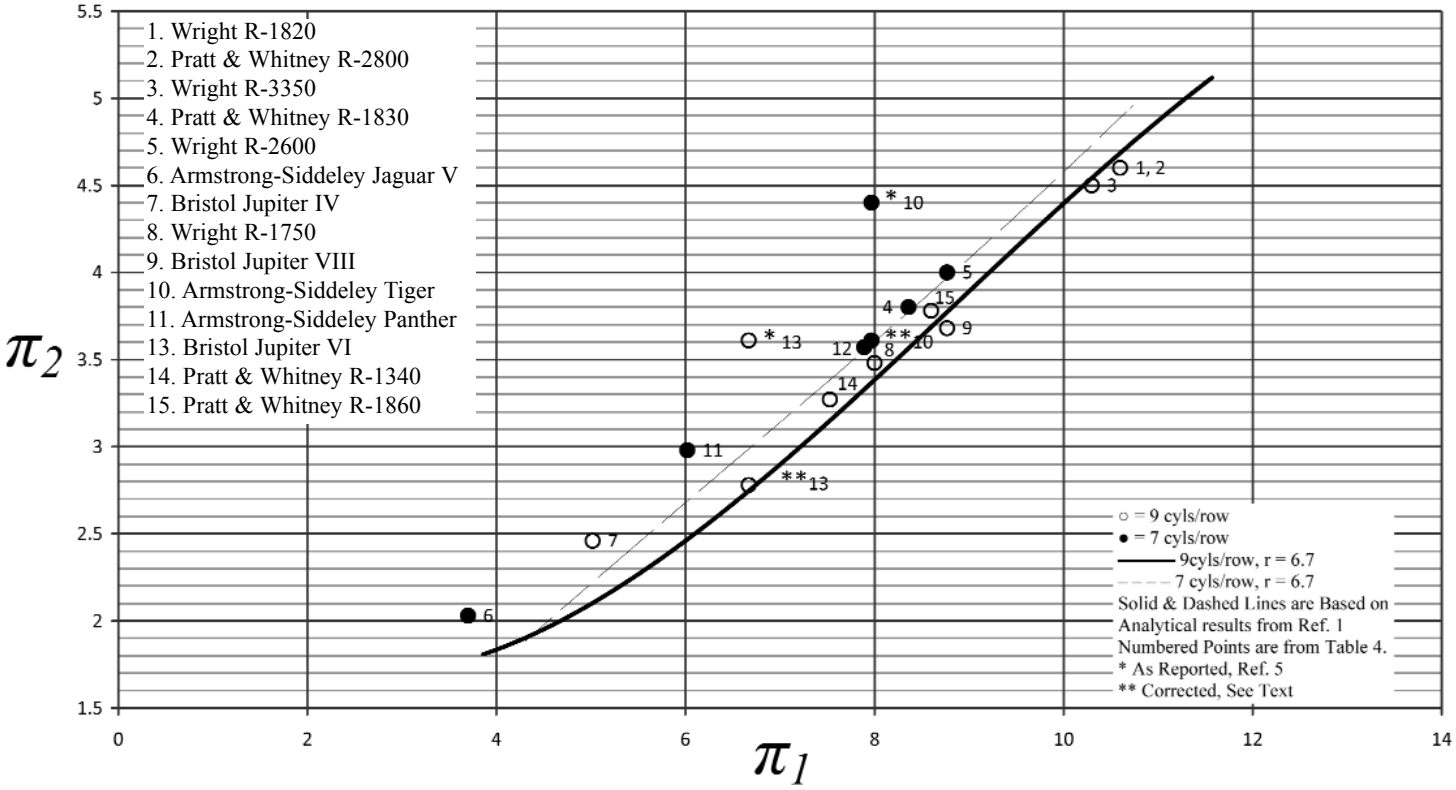

Figure 19. Dimensionless Maximum Bearing Load versus Dimensionless Mean lnertia Load, Radial Engines

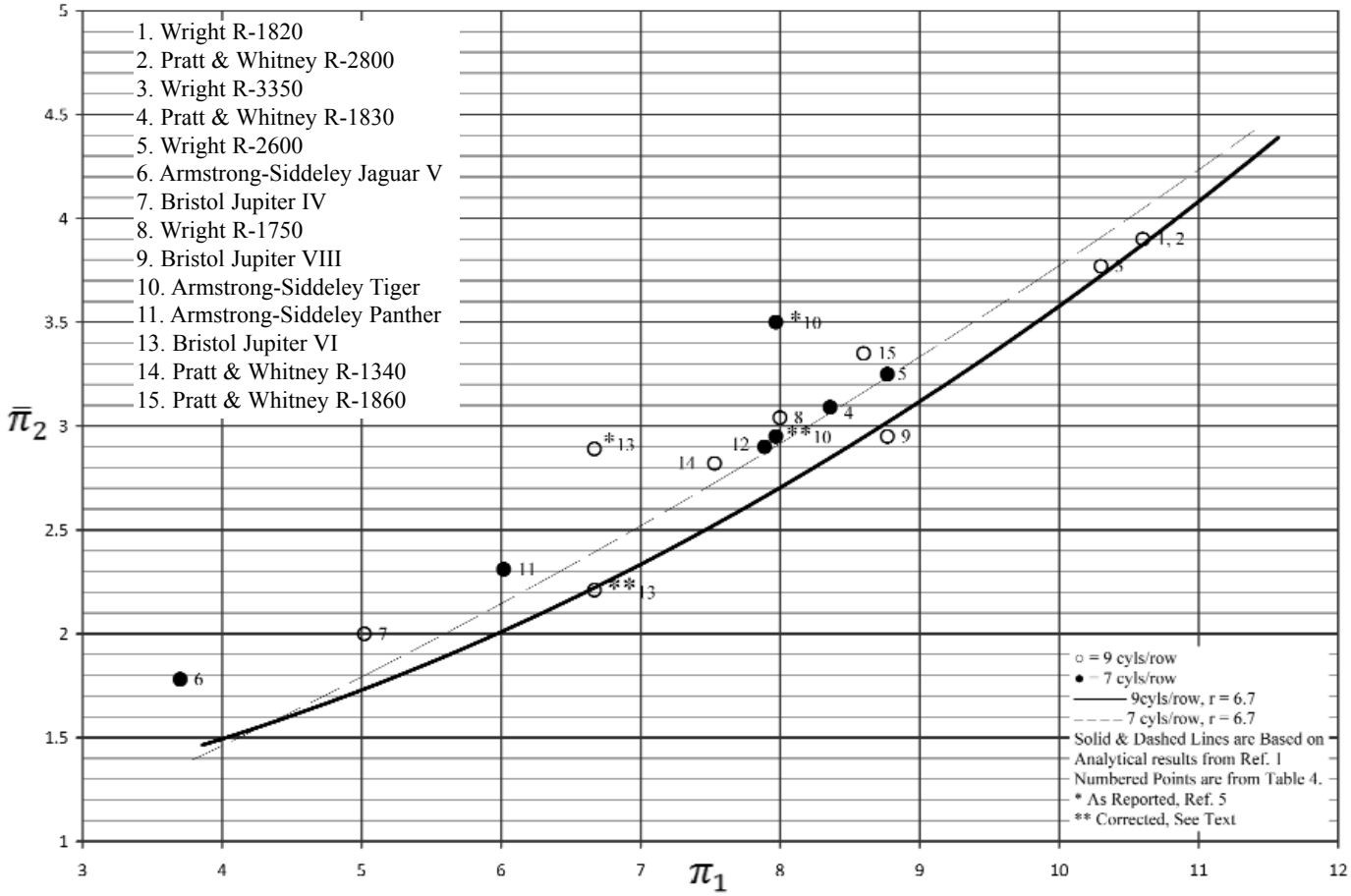

Figure 20. Dimensionless Mean Bearing Load versus Dimensionless Mean Inertia Load, Radial Engines

Table 5. Maximum and Mean Crankpin Bearing Loads
Merlin 130 and Allison V-1710
3,000 RPM and 336 psi
Indicated Mean Effective Pressure

Engine	Brake Horsepower BHP	Compression Ratio r	Max Load W (lb)	Mean Load $\overline{W}$ (lb)	Max Unit Pressure p_{MAX} (psi)	Mean Unit Pressure $\overline{p}$ (psi)	Remarks
Merlin 130	1645	6.0	18853	10092	3398	1819	Maximum loads calculated by Author. Mean loads calculated by method outlined in text section "Bearing Load Analysis - In-Line Engines"
Allison V-1710	1707	6.65	19584	12197	3365	2096	
Allison V-1710 (lowered compression ratio)	1707	6.0	17787	12197	3056	2096	

Table 6. Comparison of Bearing Loads in Radial Engines, 9 versus 7 cylinders
Based on the Wright R-1820 (Engines 1 & 12, Tables 2 & 4) @ 2,800 RPM & 286 psi
Indicated Mean Effective Pressure

		Max Load W (lb)	Mean Load $\overline{W}$ (lb)	Remarks
Number of Cylinders	9	49,356	41,845	Assumes the Crankpin Dimensions are Unchanged
	7	42,489	34,334	

Most radial engines had bore/stroke ratios of less than one. The question naturally arises as to whether the choice of this ratio was made on the basis of bearing loads or another important variable, the diameter of the engine. I have explored the question of engine diameter in Reference 32 where it was shown that engine diameter was a minimum at a bore/stroke ratio of about 0.9 for 9 cylinders per row and about 1.15 for 7 cylinders per row. Both values depend on assumptions about the design ratios of the engine, including master rod to stroke ratio, piston length to bore ratio, etc. but despite this potential for reduced frontal area, no seven cylinder per row radial had a bore/stroke ratio greater than one although the seven cylinders per row engines of Wright, Pratt & Whitney and Bristol all had larger bore/stroke ratios than their 9-cylinder counterparts (see Table 2). The reason for this may be apparent from a look at Figure 21, where I have plotted maximum bearing pressure versus bore/stroke ratio. The assumptions made in developing these curves are given on the figure. The relationships between knock limited imep and bore size were developed from material in (31). Figure 21 indicates that the bore/stroke ratio chosen for these two nine-cylinders-per-row engines minimizes the bearing pressure while keeping the engine diameter at an optimal value.

Given the importance of frontal area and bearing loads it seems reasonable to assume that design studies by the

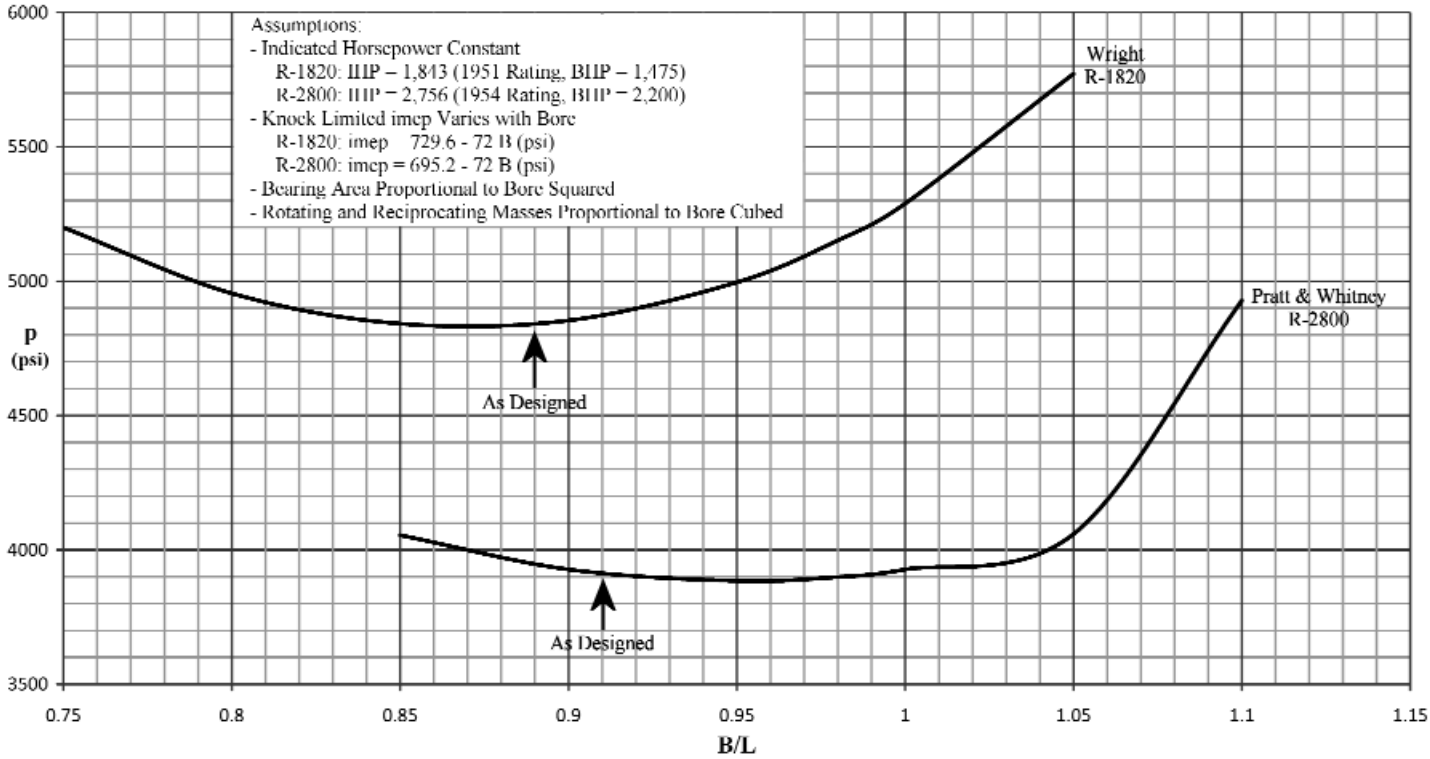

Figure 21. Maximum Crankpin Bearing Pressure versus Bore/Stroke Ratio, Two Radial Engines

engine manufacturers explored these issues in great detail, especially toward the end of the large piston engine era.

This is another example of the power of dimensional analysis. By getting the equations of the lines for dimensionless bearing loads from Figure 19 the engine dimensions and weights are defined by the dimensionless groups that make up the relationship and the task of creating Figure 21 is greatly simplified.

A Variation on a Theme

Most in-line and radial crankpin bearings were clamped or pressed into the connecting rod, and oil was introduced through a passage drilled in the crankpin. The radial engine master rod shown in Figure 1 (a Wright design) adopted a floating bearing that was prevented from rotating by the set of teeth on the left end and a mating set in the knuckle-pin locking plate also shown in Figure 1. According to Reference 1 the clearance between the outer diameter of the bearing and the inner diameter of the master rod was about 0.003". This type of arrangement also lends itself to interchangeability since the vagaries of press fits are eliminated. It also makes the bearing less sensitive to the effects of bending in the crankshaft, distortion of the big end of the master rod by the articulated rod loads, and misalignment due to crankcase deflections. A rather elegant solution to a number of potential problems.

Bristol

Bristol deserves a special section because, as in so many other aspects of aircraft engine design, they were often out of the main stream in the area of crankpin bearings.

Figure 22 shows an interesting early attempt by Bristol to reduce or eliminate the rotating crankpin bearing inertia load and possibly some of the reciprocating load as well. Two counterweights were attached to the big end of the rod but were free to rotate relative to the rod and were guided in slots on the normal crank counterweights. These were apparently installed on the Jupiter II according to the 1920 Jane's but are not mentioned in the 1922 issue. These sliding counterweights would also have reduced the size of the fixed counterweights.

One would expect that Roy Fedden would have had a better idea and, as with many other aspects of aircraft engine design, he doesn't disappoint on the subject of crankpin bearings. This account is from Ricardo (22). Ricardo's firm was approached by Bristol and the British Air Ministry to help in solving a crankpin bearing problem in the Jupiter engine. This was in "1922-1923" and the bearings were apparently failing from excessive temperature. Ricardo states there was "a maximum oil flow that could be tolerated" because their oil control piston rings were not able to handle the oil thrown off the master rod when that "maximum flow" was exceeded. Based on some previous experience with steam turbines using a fully floating bearing, Ricardo designed a "freely perforated floating bush". This apparently worked well enough in the one-piece master rod used in Ricardo's test fixture but not so well in the split rod, presumably because the floating bushing would have had to have been split as well. Since the split rod was standard in the Jupiter at that time, this was apparently what led to the one piece master rod and built-up crankshaft at Bristol (see the Jupiter engines in Table 2 and discussion above on rotating weights). It is difficult to understand how a floating bushing with a large number of holes could allow an adequate hydrodynamic film to develop. Figure 23 shows a floating bushing in an early Hercules crank assembly. Note that the Bristol bushing was allowed to freely rotate, unlike the Wright bushing described above.

In any case the floating bush was eventually abandoned by Bristol. According to Banks (23) Bristol's Polish licensee (P.Z.L.) for the Pegasus engine convinced Fedden to go back to a fixed bearing. Bristol went back to a fixed bearing but they didn't press it into the master rod, instead they shrank it to the crankpin as shown in Figure 24.

This required a passage through the bearing to communicate with the journal surface, now the inner diameter of the

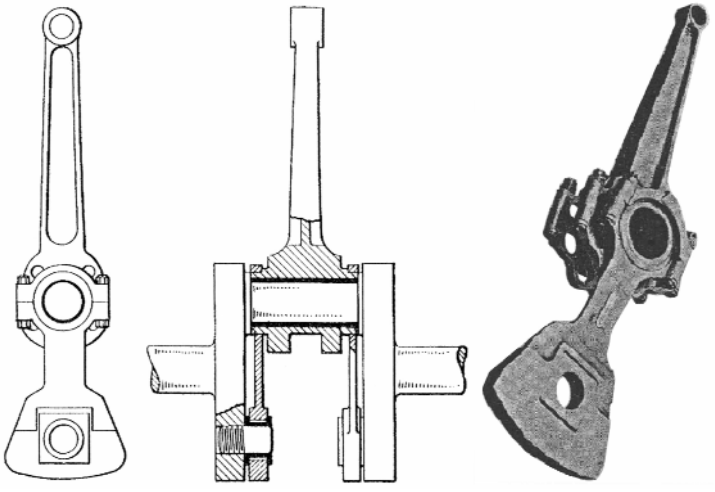

Figure 22. Bristol Jupiter Connecting Rod Big-End Balancing Counterweights

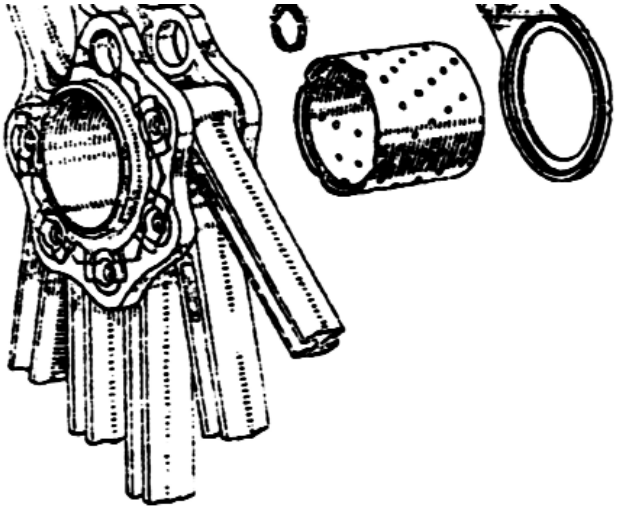

Figure 23. Early Bristol Hercules Connecting Rod Assembly Showing Perforated Floating Bushing

master rod. As Figure 24 indicates, they went to fairly elaborate lengths to spread the oil over the bearing surface. The slot in the crankpin in the view without the bearing in place looks like it could be a significantly higher stress riser than a simple hole and the elaborate sculpting on the bearing surface reduces the effective bearing area which, as we will see, doesn't really matter in the case of radial engines. The really striking thing is that, while their competitors were adopting silver-lead-indium bearings, Bristol adopted a tin based Babbitt (white metal). How did they get away with this? I puzzled over this for some time until David Robinson (R-RHT member) came up with Reference 33 by Markham of Bristol. By making the bearing surface the outer diameter of the crankpin rather than the inner diameter of the master rod the load profile is restricted to about 140° of the circumference of the crankpin rather than 360° if the bearing were located in the master rod. This apparently reduced the stress range enough so that the bearing would not fail from fatigue.

In order to verify this claim I analyzed the crankpin loads of the Wright R-1820 using Figure 18 to get the bearing loads and vector orientations and then transformed them relative to the crankpin and master rod. The result is shown in Figure 25, and shows the load vectors oscillating 70° on either side of the crankpin axis while they traverse the entire master rod inner diameter circumference. So the bearing load varies from 37,000 lb to zero on the master rod but 37,000 to 31,000 lb on the crankpin, a much reduced range. This is somewhat of a simplification since these loads are supported by an oil film whose maximum pressure is also oscillating in a similar manner but apparently it does not drop to zero over the range shown in Figure 25.

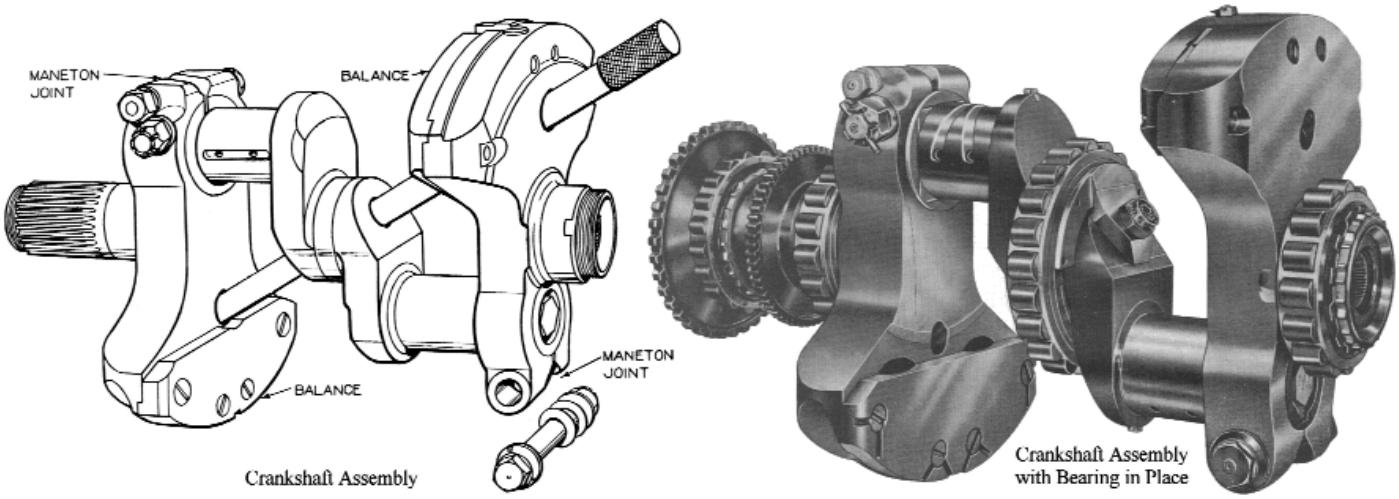

Figure 24. Bristol Crankpin Bearing

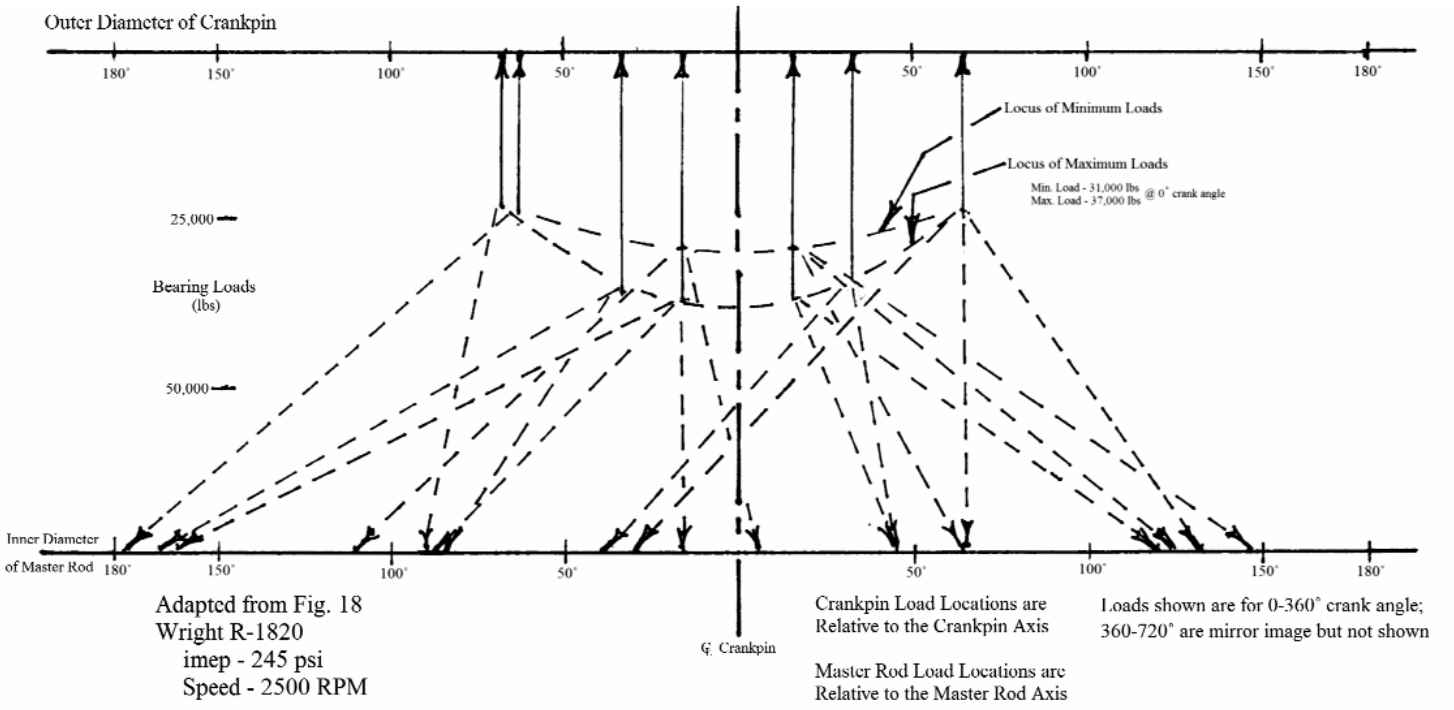

Figure 25. Crankpin Bearing Load Pattern versus Crank Angle

This result also indicates why the elaborate sculpting shown in Figure 24 is not a detriment to bearing performance since it is in an area of the crankpin that is always unloaded. It was apparently adopted to increase the oil flow through the bearing and keep bearing temperatures down, which would also increase the fatigue resistance of the bearing. Reference 34 describes tests on the effects of oil grooves on bearing performance and a configuration very similar to that shown in Figure 24 was shown to give three to four times the flow of a simple hole.

Given that Babbitt is a superior bearing material in many respects save fatigue strength, it seems very odd that in all of the work carried out by the NACA the technique adopted by Bristol was, to my knowledge, never mentioned as a possibility and certainly not adopted by any major American manufacturer. Since most late radial engine designs utilized built-up crankshafts any crankpin bearing change required that the crankshaft be disassembled so the fact that Bristol's bearing was shrunk onto the crankpin would not have made much difference in repair time.

Crankpin Bearing Lubrication

All engines described in this paper had pressure lubricated crankpin and main bearings. Oil was supplied either directly to the crankshaft or through an oil gallery to the main bearings and from there to the crankpin. The lube oil serves to establish a film that prevents metal to metal contact between the journal and bearing and to provide cooling. The splash system that persisted in automotive practice for a number of years could not provide an oil flow rate that was adequate to keep the bearing temperature at an acceptable level in the higher specific power ratings of aircraft engines.

The variables that affect the flow rate of oil are: supply pressure, bearing clearance, and the length to diameter ratio of the bearing. The clearance and the length to diameter ratio are under the control of the designer and require a very tricky balance between oil flow rate and minimum oil film thickness. The flow rate increases as the cube of the clearance but the minimum film thickness decreases approximately linearly with clearance. If a bearing is limited by temperature an increase in clearance can help, but if it is limited by minimum film thickness a decrease in clearance can help.

These trade-offs are shown in Figure 26, which is based on the geometry and running conditions of the Wright R-1820 ca.1951. Data from Reference 24 was used to calculate the flow rates and minimum film thickness shown. The trade-off between flow rate and film thickness is apparent. The effect of length to diameter ratio is included to show how a designer confronted with a bearing problem might react to, say, an inadequate oil film thickness. If he decreases the clearance and then runs into a temperature problem because of a reduction in oil flow he can shorten the bearing to try to regain some of the lost flow rate. We have noted how (Figs. 2 and 3) the bearing length to diameter ratio decreased over time and the reasons for that change. The effects of shaft deflection also play an important role in the selection of bearing clearance and an increase in clearance

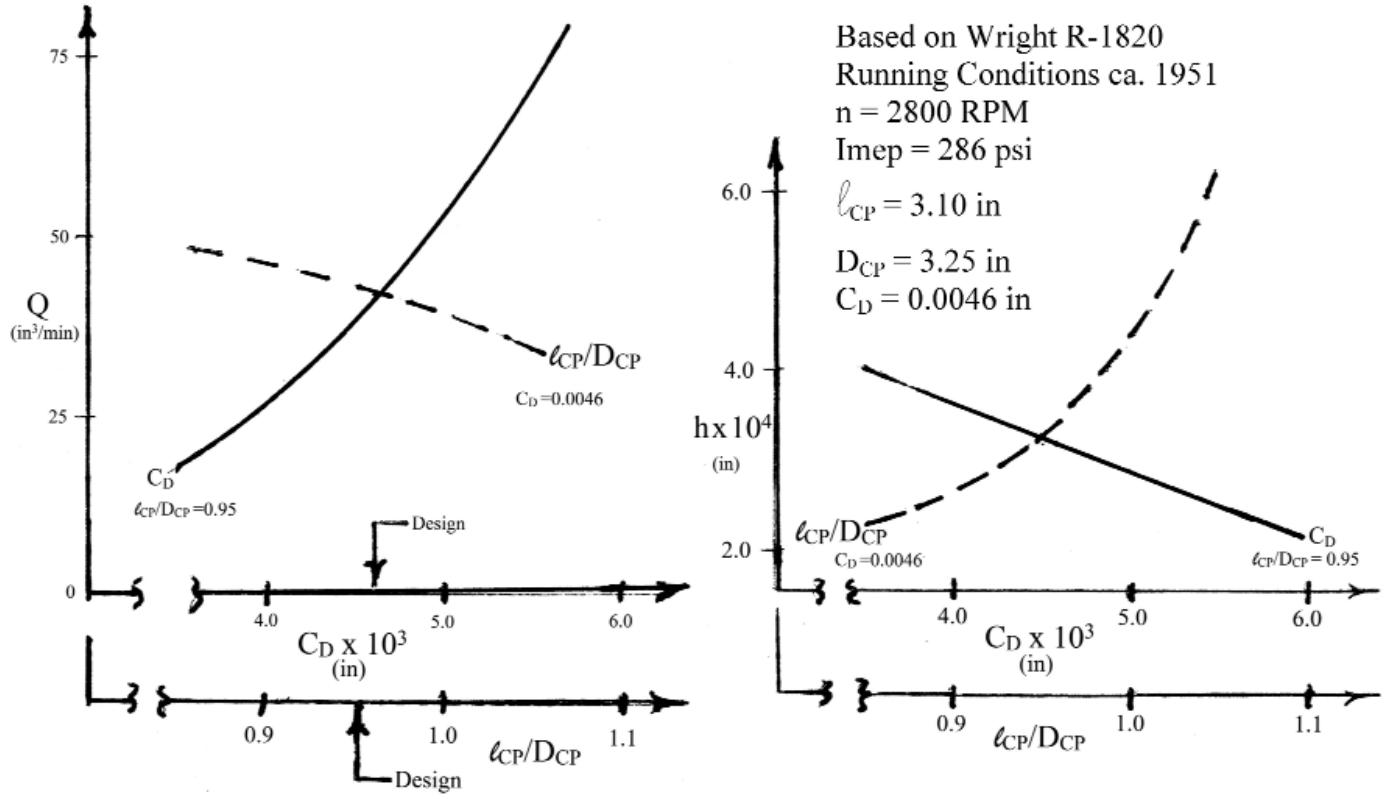

Figure 26. Crankpin Oil Flow and Minimum Film Thickness versus Bearing Clearance and Bearing Length to Diameter Ratio

to solve a wear problem due to deflections cannot be carried out without consideration of the other variables concerned.

All of the crankpin bearings of the engines discussed here had oil supplied through passages in the crankpin. In most cases this was a simple hole from the hollow crankpin to the surface of the journal, the Bristol engines just discussed being the only exceptions. The question of where to position the hole relative to the crank axis was important. In order to maximize the oil flow the hole should be positioned where the average oil film pressure is a minimum. For radial engines this is a relatively simple matter because, as Figure 25 indicates, there is a large fraction of the circumference of the crankpin that is not loaded and the oil hole can be placed anywhere in that area. Most engines put the hole on the crank axis to take advantage of the centrifugal force, which can double the pressure at 2,500 rpm in a typical engine.

In the case of in-line engines the solution is not so simple because, unlike the radial engine, there typically is nowhere that is always unloaded so the next best thing is to have the oil hole where the loads are lightest for the shortest period of time. This involves creating a force diagram relative to the crank axis and determining the area where the time-weighted load is a minimum. This procedure is demonstrated in (1) for the Allison V-1710 at 3,000 rpm and 242 psi imep. The result for the optimum oil hole position was at an angle of 70° to the crank axis in the direction of engine rotation. Reference 10 shows an un-dimensioned, sectioned, crankpin for the V-1710 with the oil hole at approximately 60° to the crank axis and a symmetrical hole on the other side of the crankpin presumably to allow one crank to be used for either rotation.

Closing Comments

It has been my purpose to show how bearing loads and bearing geometry changed over the period 1915-1950. Perhaps the most striking thing about these results is the progression from the broad range of values of the design ratios in the early years to a fairly narrow consensus in the final years as exhibited in Figs.2, 3, & 4. I had suspected that this would be the case but was surprised at the magnitude of the differences in the earlier years. It was also gratifying to note that an outlier like the Curtiss V-1570 was a troublesome engine with regard to bearing failures. It indicates what can happen if you attempt to push the envelope too far too soon.

The maximum bearing pressures for in-line and radial engines ended the period at about the same level, the Rolls-Royce Griffon pressure being slightly higher than the highest radial (Fig.5) and this also came as a surprise. The minimum oil film thickness for the radials at the end of the era was somewhat below the in-line engines primarily due to the higher mean bearing loads.

In support of my contention that aircraft engine bearing development led to much of the bearing technology currently in use in all piston engines, I submit the steel-backed aluminum bearing so prevalent today. Rolls-Royce was considering them as early as 1940 and the NACA was sponsoring development of them in the mid 1940's.(36,37)

Heron (Reference 19) has claimed that plain bearings save weight and, at least according to Val Cronstedt (19), are more reliable. As I mentioned in the text, the Daimler-Benz 601A utilized a 3 row roller bearing with a duralumin cage (Ref.35). Since the crankpin diameter to bore ratio at 0.57 is well above the average for the period (see Fig.2) it is fairly safe to assume that the resulting rotating weight is significantly higher than it would have been with a journal bearing. We can compare the weights of the DB-601A with the Jumo 211B, a very similar engine and from the same country: the DB-601A weighed 0.76 lbs./in^3 of displacement while the Jumo-211B weighed 0.67, a fairly significant difference. The weight per take-off horsepower was slightly higher for the DB engine as well.

With regard to air-cooled engines, the closest we can come to a journal versus rolling element weight comparison is between the Pratt & Whitney R-2800 (so far as I am aware the only radial engine with journal main bearings in all positions) and the Wright R-2600 with rolling element bearings in all main bearing positions. The R-2600 is lighter on a per cubic inch basis (0.79 versus 0.84) and slightly heavier on a horsepower basis (1.07 versus 0.98). I am not sure this tells us very much about the relative effects of bearing type since the design philosophies of the two engines were probably significantly different in other respects.

Finally, I would like to make the case for some systematic approach to obtaining pertinent engine information. In the course of writing this paper I have become quite conscious of the fact that, as the Acknowledgement section amply demonstrates, the only source of dimensions and weights is through the generosity of people who have engines disassembled and are willing to take the time to measure or weigh the relevant parts. I could hardly believe that the reciprocating and rotating weights of the Merlin were not published somewhere, but apparently they are not. I have not been able to find much of the material needed on the later Bristol engines except from people who have one in parts. My own particular interests, as anyone who has read this paper and my previous papers will be aware, lie on the analytical side. I don't know if this particular approach to engine history will outlive me, but I hope others will see the importance of this technique for gaining an understanding of why and how certain design decisions were made in the course of developing these magnificent examples of the art of mechanical engineering.

I have had to resort to scaling dimensions of pistons, valves, crankshafts. etc., from transverse and longitudinal cross-sectional drawings on numerous occasions from knowing only the bore and stroke of the engine in question. I suppose we are lucky to have these available but I am always worried that the drawings I am scaling from have been distorted when placed in the journals where they appear. Perhaps we could, as an organization and teamed

with similar organizations, establish a data base of the important engines listing critical dimensions and weights. Members could then submit what they know about specific engines and organizations that rebuild these engines could be asked to provide information.

Acknowledgements

I have had a great deal of help from many people who took the time to search out data sources and weigh engine parts. Kim McCutcheon obtained the Merlin weights for me from an engine re-builder and steered me to information on the Curtiss V-1570. Tom Fey weighed his Griffon rods for me and Brian Mills supplied the Griffon piston weights, thus making it possible to include the last significant in-line, liquid cooled engine in this paper. Brian also supplied all of the Bristol Centaurus reciprocating and rotating weights, which allowed a comparison of late model American and British radial engines that otherwise would have been missing from this report. Barry Hares provided Rolls-Royce Eagle 22 crankpin dimensions. Special thanks to Conor Rachlin for his assistance in preparing charts and tables.

David Robinson has kindly offered advice and supplied the key paper which explained what had been a great mystery to me; how Bristol got away with Babbitt bearings. He also reviewed a draft of this paper and provided many valuable insights and comments.

References

1. Shaw, M.C. & Macks, E.F. *Analysis and Lubrication of Bearings*. McGraw-Hill Book Co., Inc., 1949.

2. Gunston, Bill. *World Encyclopedia of Aero Engines, 3rd edition*. Patrick Stephens Ltd.

3. Lumsden, A. *British Piston Aero Engines and their Aircraft*. Airlife, England.

4. Prescott, F.L., & Poole, R.B. "Bearing Load Analysis and Permissible Loads as Affected by Lubrication in Aircraft Engines", *S.A.E. Transactions* v.26, 1931.

5. Swan, A. *Handbook of Aeronautics, v.II, Aero Engines Design and Practice*. Sir Isaac Pitman & Sons, Ltd., London, 1934.

6. Angle, Glenn D. *Engine Dynamics and Crankshaft Design*. 1925.

7. Samuels, W. *Engine Bearing Loads*. Edwards Bros., Ann Arbor, MI, 1935.

8. Schlaifer, *Robert & Heron, S.D. Development of Aircraft Engines and Fuels*. Harvard University School of Business Administration, Cambridge, MA, 1950.

9. Swan, A. *Piston and Connecting Rod Weights and Other Related Data in Modern Aircraft Engines*. R&M 1300, Sep 1925.

10. Shaw, M. C. & Macks, E. F. "In-Line Aircraft Engine Bearing Loads, I, Crankpin Bearing Loads", *NACA ARR No. E5H10a*. Oct 1945.

11. Shaw, M. C. & Macks, E. F. "Radial Aircraft-Engine Bearing Loads, I, Crankpin Bearing Loads for Engines Having Nine Cylinders per Crankpin", *NACA ARR E5H04*. Oct 1945.

12. "Rolls-Royce Eagle", *Flight*. 24 Apr 1947.

13. "Rolls-Royce Griffon (65)", *Flight*. 20 Sep 1945.

14. Frey, M. L. "The Metallurgy and Processing of the Packard-Built Rolls-Royce Merlin Crankshaft". *Proceedings of the Society of Experimental Stress Analysis* vol. II, no.2, 1944, p.158.

15. Custer, J. "Aeronautical Engineering, America's Trump Card", *Automotive and Aviation Industries*. 1, 15 Apr 1942.

16. *Jane's All the Worlds Aircraft*. Arco Publishing Co. N.Y., 1919.

17. "Centaurus Aircraft Engine", *Automotive Industries*, 15 Sep1945.

18. "Pistons of American, British, French and Russian Aircraft Engines", *Automotive and Aviation Industries*. 15 Sep 1944. (This article was prepared from a British Ministry of Aircraft Production translation of the report "Design Characteristics of Modern Enemy Aero-Engine Pistons" by H. Schwarz and published in *Luftwiessen*, No date given.)

19. Heron, S. D. *History of the Aircraft Piston Engine*. The Ethyl Corporation, 1961.

20. Whitney, Daniel D. *Vee's For Victory! the Story of the Allison V-1710 Aircraft Engine, 1929-1948*, Appendix 10. Schiffer Publications, Atglen, PA.

21. *The Pratt & Whitney Story*. Pratt & Whitney Division of United Aircraft Corp., 1950.

22. Ricardo, Sir Harry. *Memories and Machines: the Pattern of my Life*. Constable, London, 1968.

23. Banks, Rod. *I Kept no Diary*. AirLife Publications.

24. DuBois, G. B., et.al.,(Cornell University), "Experimental Investigation of Eccentricity Ratio, Friction, and Oil Flow of Long and Short Journal Bearings with Load Number Charts", *NACA TN 3491*. Sep 1955.

25. Hourwich, I. & Foster, W. J. *Air Service Engine Handbook*. Engineering Division, U.S. Army Air Service, McCook Field, Dayton, Ohio,1925.

26. Marks, L. S. *The Airplane Engine*. McGraw-Hill, New York, 1925.

27. Royal Aircraft Establishment R&M 1486, Sept,1931.

28. Wilkinson, Paul H. Aircraft Engines of the World. New York. 1946.

29. Massachusetts Institute of Technology, Institute Archives & Special Collections, Manuscript Collection-MC71. Charles Fayette Taylor Papers 1917-1973, Box #9, Folder 43A.

30. Edson, M. H. & Taylor, C.F., "The Limits of Engine Performance-Comparison of Actual and Theoretical Cycles", *S.A.E., Digital Calculations of Engine Cycles, Progress in Technology*, v7. 1964.

31. Taylor, C.F. *The Internal Combustion Engine in Theory and Practice*, vol.2, Fig.2-35. M.I.T. Press, Cambridge MA.

32. Raymond, R. "Comparison of Sleeve Valve and Poppet Valve Aircraft Engines". AEHS, April, 2005. http://www.enginehistory.org/members/articles/Sleeve.pdf.

33. Markham, B.G. "Air Cooled Engines", *Flight*, 28 Sep 1944.

34. Clayton, D. "An Exploratory Study of Oil Grooves in Plain Bearings". The Institution of Mechanical Engineers, 1946, 155:41.

35. Young, R.M. "Mercedes-Benz DB-601A Aircraft Engine", *S.A.E. Journal (Transactions)*, V49, N2. Oct 1941.

36. Hives, E.W.& Smith, F. "High Output Aero Engines", *Aircraft Engineering*. July, 1940, p.194.

37. Macks, E. F. & Shaw, M. C. "Load Capacity of Aluminum-Alloy Crankpin Bearings as Determined in a Centrifugal Bearing Test Machine", *NACA Technical Note 1108*. Aug 1946.

Definitions and Derivations

B = Bore

C_D = Diametral Bearing Clearance

D_{CP} = Crankpin Diameter

$\frac{D_{CP}}{C_D}$ = 700 for Radial Engines; 1333 for In-Line, V and W Engines

e = Distance Between Crankpin and Crankpin Bearing Centers

f = Friction Coefficient

g = Acceleration due to Gravity

$h_{min} = \frac{C_D}{2}(1-n)$ = Oil Film Thickness

$imep$ = Indicated Mean Effective Pressure

K = A Constant Derived from Analysis (See Fig. 14)

L = Stroke

l_{CP} or ℓ_{CP} = Crankpin Length

l_{CR} or ℓ_{CR} = Master Rod Length

$M_e = (W_{ROT} + KW_{RCP})/g$ = Equivalent Mass to Give Same Mean Inertia Load, In-Line Engines

$M_e = \left\{ W_{ROT} + \left[\frac{1}{2} + \frac{1}{4}\left(\frac{L}{2\ell_{CR}} \right)^2 \right] W_{RCP} \right\} \Big/ g$ = Equivalent Mass to Give Same Mean Inertia Load, Radial Engines

N = revolutions per minute

n = Number of Cylinders

$n = \frac{2e}{C_D}$ = Crankpin Eccentricity Ratio

p = Crankpin Bearing Unit Pressure

Q = Oil Flow

r = Compression Ratio

$S_o = \left(\frac{D_{CP}}{C_D} \right)^2 \frac{\mu N}{\bar{p}}$ = Sommerfeld Number (See Tables 3 & 4)

W = Peak Bearing Load

W_e = Effective Weight to Give Mean Inertia Load = $M_e g$

W_{RCP} = Total Reciprocating Weight per Crankpin

W_{ROT} = Total Rotating Weight per Crankpin

$\bar{W}$ = Mean Crankpin Bearing Load

μ = Oil Viscosity

$\pi_1 = \frac{M_e N^2 L}{B^2 imep}$

$\pi_2 = \frac{W}{B^2 imep}$

$\bar{\pi}_2 = \frac{\bar{W}}{B^2 imep}$

Figure 27. Definitions and Derivations